

AD-A039 519

AEROSPACE CORP EL SEGUNDO CALIF ENGINEERING SCIENCE --ETC F/G 3/1  
A 'BLIND' STAR IDENTIFICATION METHOD.(U)  
APR 77 R 6 NISHINAGA

UNCLASSIFIED

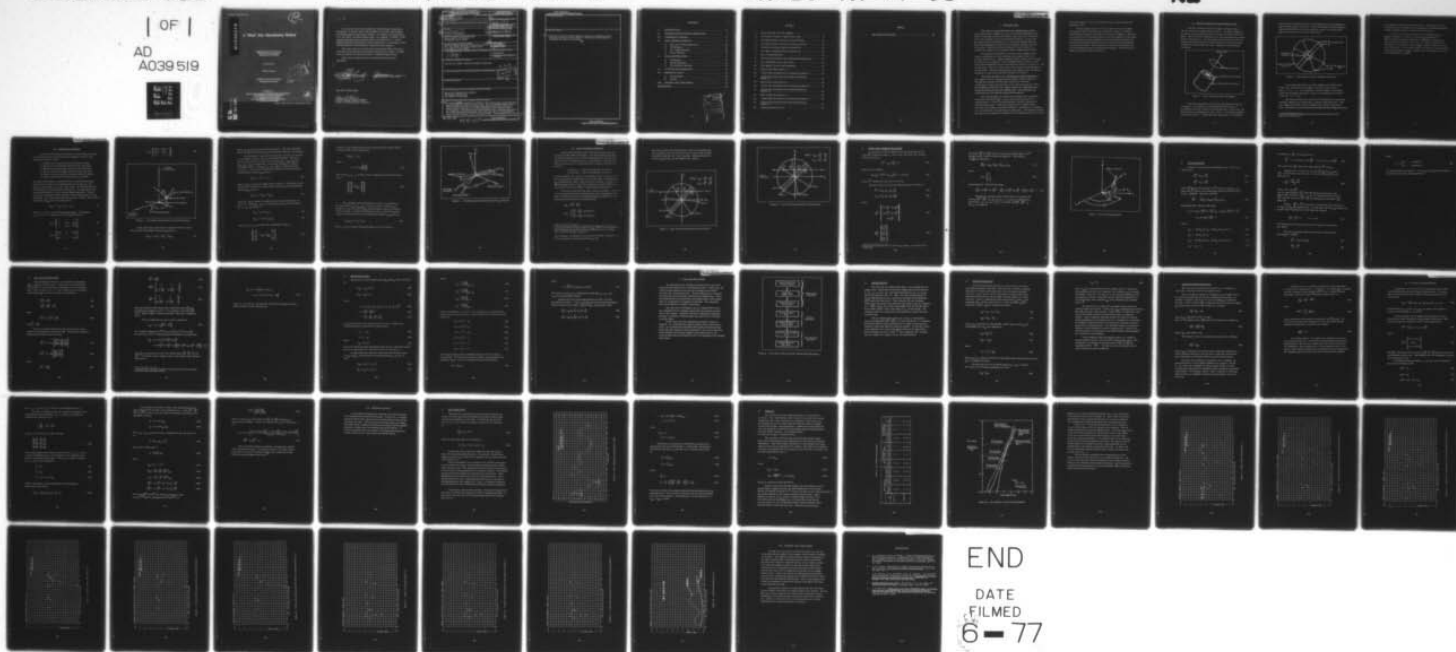
TR-0077(2901-03)-2

SAMSO-TR-77-93

F04701-76-C-0077  
NL

| OF |

AD  
A039 519



ADA 039519

12  
NW

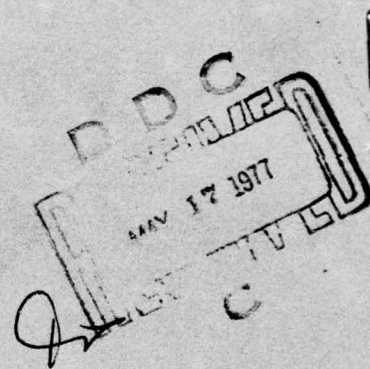
## A "Blind" Star Identification Method

Engineering Science Operations  
The Aerospace Corporation  
El Segundo, Calif. 90245

14 April 1977

Interim Report

APPROVED FOR PUBLIC RELEASE:  
DISTRIBUTION UNLIMITED



Prepared for  
SPACE AND MISSILE SYSTEMS ORGANIZATION  
AIR FORCE SYSTEMS COMMAND  
Los Angeles Air Force Station  
P.O. Box 92960, Worldway Postal Center  
Los Angeles, Calif. 90009



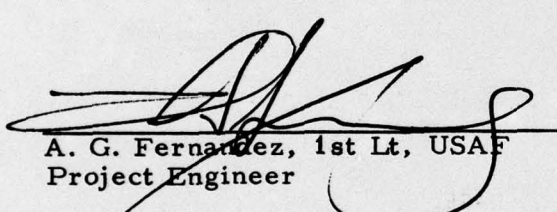
THE AEROSPACE CORPORATION

AD NO. \_\_\_\_\_  
DDC FILE COPY,

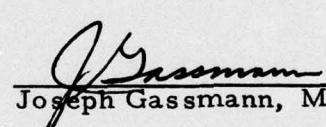
This interim report was submitted by The Aerospace Corporation, El Segundo, CA 90245, under Contract F04701-76-C-0077 with the Space and Missile Systems Organization (AFSC), Los Angeles Air Force Station, P. O. Box 92960, Worldway Postal Center, Los Angeles, CA 90009. It was reviewed and approved for The Aerospace Corporation by D. J. Griep, Engineering Science Operations. First Lieutenant A. G. Fernandez, YAPT, was the Deputy for Advanced Space Programs project engineer.

This report has been reviewed by the Information Office (OI) and is releasable to the National Technical Information Service (NTIS). At NTIS, it will be available to the general public, including foreign nations.

This technical report has been reviewed and is approved for publication.



A. G. Fernandez, 1st Lt, USAF  
Project Engineer



Joseph Gassmann, Maj, USAF

FOR THE COMMANDER



Floyd R. Stuart, Colonel, USAF  
Deputy for Advanced Space Programs



UNCLASSIFIED

SECURITY CLASSIFICATION OF THIS PAGE (When Data Entered)

19 REPORT DOCUMENTATION PAGE		READ INSTRUCTIONS BEFORE COMPLETING FORM	
1. REPORT NUMBER SAMSOTR-77-93	2. GOVT ACCESSION NO.	3. RECIPIENT'S CATALOG NUMBER	
4. TITLE (and Subtitle) A BLIND STAR IDENTIFICATION METHOD.		5. TYPE OF REPORT & PERIOD COVERED Interim rept.	
7. AUTHOR(s) Ronald G./Nishinaga		6. PERFORMING ORG. REPORT NUMBER TR-0077(2901-03)-2	8. CONTRACT OR GRANT NUMBER(s) F04701-76-C-0077
9. PERFORMING ORGANIZATION NAME AND ADDRESS The Aerospace Corporation El Segundo, Calif. 90245		10. PROGRAM ELEMENT, PROJECT, TASK AREA & WORK UNIT NUMBERS	
11. CONTROLLING OFFICE NAME AND ADDRESS Space and Missile Systems Organization/YAPT P.O. Box 92960, Worldway Postal Center Los Angeles, Calif. 90009		12. REPORT DATE 14 Apr 1977	
14. MONITORING AGENCY NAME & ADDRESS (if different from Controlling Office) 1264p.		13. NUMBER OF PAGES 63	
		15. SECURITY CLASS. (of this report) Unclassified	
		15a. DECLASSIFICATION/DOWNGRADING SCHEDULE	
16. DISTRIBUTION STATEMENT (of this Report) Approved for public release; distribution unlimited.			
17. DISTRIBUTION STATEMENT (of the abstract entered in Block 20, if different from Report)			
18. SUPPLEMENTARY NOTES			
19. KEY WORDS (Continue on reverse side if necessary and identify by block number) Spacecraft Attitude Determination Parameter Identification Star Mapper Processing			
20. ABSTRACT (Continue on reverse side if necessary and identify by block number) A method <sup>was</sup> <del>has been</del> developed to identify a set of stars that crossed the slits of star mappers located on a spacecraft. The star identification problem is <sup>is</sup> <del>is</del> blind in the sense that the inertial orientation of the spacecraft is not known and the particular set of slits generating transit measurements is not designated. Utilizing transit measurements from a spinning spacecraft, the method identifies the unknown set of slits and stars by processing the measurements through a series of decision tests. Once identified, the star			

DD FORM 1473  
(IFACSIMILE)

UNCLASSIFIED

SECURITY CLASSIFICATION OF THIS PAGE (When Data Entered)

404 068

AB

next page

DDC  
RECEIVED  
MAY 17 1977  
C



UNCLASSIFIED

SECURITY CLASSIFICATION OF THIS PAGE(When Data Entered)

19. KEY WORDS (Continued)

20. ABSTRACT (Continued)

cont. → data can be used via a least-square procedure to determine a gross estimate of the spacecraft's attitude. Numerical results based on simulated star data are presented.



UNCLASSIFIED

SECURITY CLASSIFICATION OF THIS PAGE(When Data Entered)

## CONTENTS

I.	INTRODUCTION .....	5
II.	SYSTEM DESCRIPTION AND ASSUMPTIONS .....	7
III.	COORDINATE SYSTEMS .....	11
IV.	STAR CROSSING GEOMETRY .....	17
	A. Basic Star Crossing Relations .....	20
	B. Slit Relations .....	23
	C. Arc Length Relations .....	26
	D. Error Relations .....	29
V.	STAR IDENTIFICATION .....	33
	A. Initialization .....	35
	B. Screen Operation .....	36
	C. Star Selection Operation .....	38
VI.	ATTITUDE DETERMINATION .....	41
VII.	NUMERICAL STUDY .....	45
	A. Run Conditions .....	46
	B. Results .....	49
VIII.	SUMMARY AND CONCLUSION .....	63
	REFERENCES .....	65

ACCESSION / der	
WHS	White Section <input checked="" type="checkbox"/>
RUC	Buff Section <input type="checkbox"/>
UNANNOUNCED	
JUSTIFICATION	
BY	
INSTRUMENTATION / RELIABILITY CODES	
DATE	AVAIL. DATE / SPECIAL

A

## FIGURES

1.	Basic Elements of the Star Mapper . . . . .	7
2.	Slit Pattern of Sensor j (Optical Axis View) . . . . .	8
3.	Coordinate System Geometry (I and O Frames) . . . . .	12
4.	Coordinate System Geometry ( $S_j$ and $L_{ij}$ Frames) . . . . .	15
5.	Three Slit Crossing Geometry (Geometry I) . . . . .	18
6.	Four Slit Crossing Geometry (Geometry II) . . . . .	19
7.	Star Crossing Geometry . . . . .	22
8.	Flow Chart of the Basic Star Identification Operations . . . . .	34
9.	Star Availability versus Day of Year . . . . .	47
10.	Star Density versus Visual Magnitude . . . . .	51
11.	Input Transit Data (Sensor 1) . . . . .	53
12.	Transit Data Passing the Screen Operation (Sensor 1) . . . . .	54
13.	Transit Data Passing the Star Selection Operation (Sensor 1) . . . . .	55
14.	Input Transit Data (Sensor 2) . . . . .	56
15.	Transit Data Passing the Screen Operation (Sensor 2) . . . . .	57
16.	Transit Data Passing the Star Selection Operation (Sensor 2) . . . . .	58
17.	Input Transit Data (Sensor 3) . . . . .	59
18.	Transit Data Passing the Screen Operation (Sensor 3) . . . . .	60
19.	Transit Data Passing the Star Selection Operation (Sensor 3) . . . . .	61
20.	Attitude Estimation Error . . . . .	62



## TABLE

1.	Star Identification Results . . . . .	50
----	---------------------------------------	----

## I. INTRODUCTION

This report is concerned with a star identification problem associated with star mappers on a spacecraft whose orientation is not known. Knowledge of spacecraft attitude can be lost after orbit injection or after unsupervised or uncontrolled maneuvers. In any case, the basic problem is that little or no a priori information exists on the inertial pointing direction of the star mappers during an observation period. Under these "blind" conditions, it is not clear how to associate the outputs of star mappers with a catalog of known stars.

The identification problem is focused on star mappers which employ a fixed pattern of slits and allow star images to pass to a common detector (e.g., a photo multiplier tube). In this case, the detector emits a series of pulses, each of which provides a measure of the star's visual magnitude and slit-crossing time relative to a clock (i.e., the transit time). However, the particular slits associated with the pulses are not known. Thus the outputs of these star mappers have an inherent ambiguity as to the slits associated with the star transits.

The report presents a star identification method applicable for star mappers with slit ambiguity under unknown attitude conditions. The approach assumes that the spacecraft can be controlled to spin about a known body axis prior to the observation period. When this condition is achieved, star mapper outputs are obtained and processed to provide slit and star identification. Once identified, the transit data are processed for attitude determination.

Star identification and attitude determination were undertaken by Kenimer and Walsh<sup>(1)</sup> for a spacecraft undergoing torque-free spinning motion. Grosh<sup>(2)</sup> generalized their results by allowing for spacecraft precession. Both works employed star mappers whose slits allow star images to individual detectors, resulting in no ambiguity as to the particular slit generating the output pulse. The proposed method generalizes their approach by allowing for slit ambiguity and by accounting

for the possibility of incorrect identification due to measurement and modeling errors.

The development begins with a description of the star mapper configuration under consideration. Coordinate systems are defined to specify the orientation of the spacecraft and star mappers. Relations describing the star crossing geometry of the star mappers are developed and specialized to predict parameters associated with the transit data. The statistics of these parameters due to measurement and modeling errors are developed. These relations are used to form the basis for star identification and gross attitude determination. A brief numerical study is presented in the final section.



## II. SYSTEM DESCRIPTION AND ASSUMPTIONS

The basic elements of the star mapper include an optical system, reticle and a photoelectric detector. As shown in Figure 1, the optical system images a field of stars onto a reticle at the focal plane. The reticle has a fixed pattern of slits that allows star images to pass to the detector. As star images are carried across the slit pattern, the detector emits a series of pulses to a processor which computes the transit time and visual magnitude corresponding to each pulse.

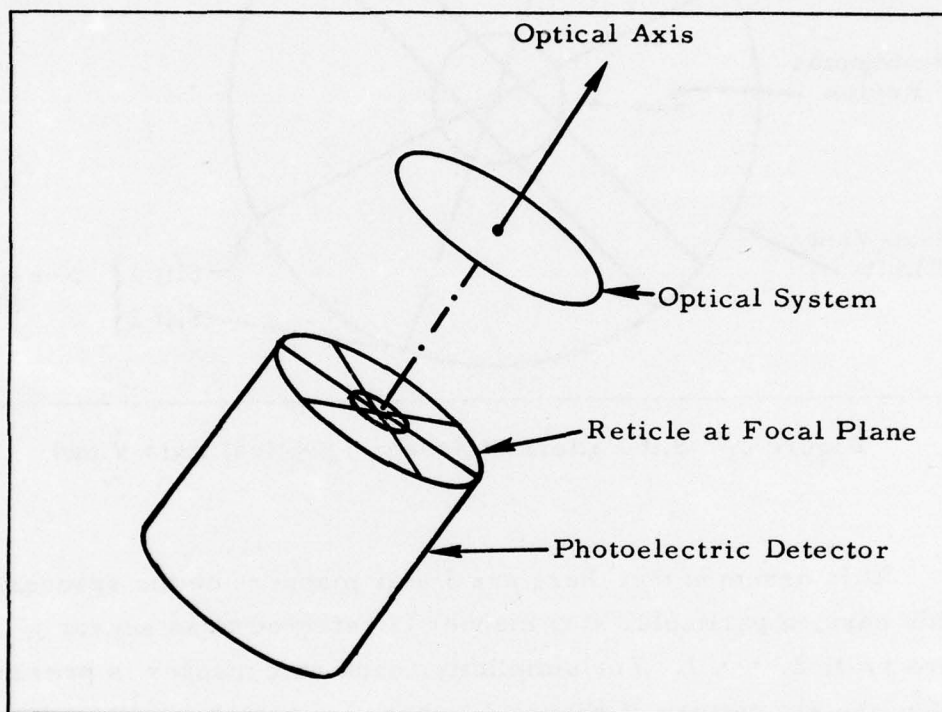


Figure 1. Basic Elements of the Star Mapper

The particular pattern of slits under consideration is shown in Figure 2. This pattern is distinguished by the presence of two parallel slits and at least one non-parallel slit. In this case, the parallel slits are designated as slits 1 and 2. To avoid the ambiguity between the slits in a region about the optical axis, it is assumed

that the detector responds only to star crossings between this ambiguous region and the field-of-view limit. Here the boundaries of the ambiguous region and the field of view are specified by circular cones whose half angles are denoted as  $F_L$  and  $F_U$ , respectively.

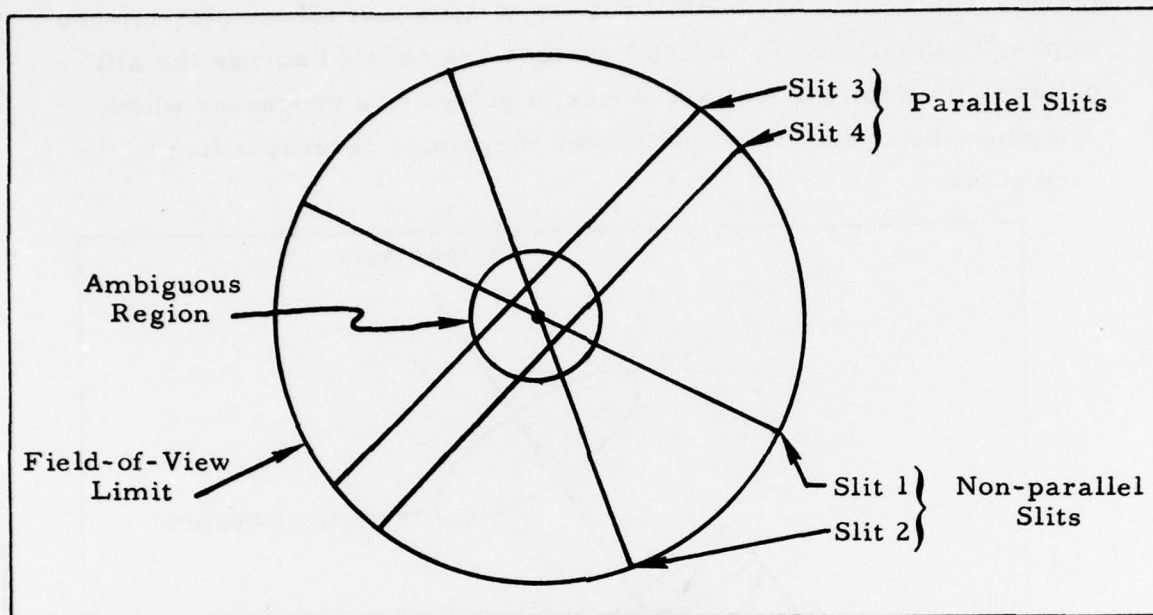


Figure 2. Slit Pattern of Sensor  $j$  (Optical Axis View)

It is assumed that there are  $J$  star mappers on the spacecraft. In this case, a particular star mapper is referred to as sensor  $j$ , where  $j = 1, 2, \dots, J$ . For simplicity, each star mapper is presumed to have the slit pattern of Figure 2, where an individual slit is denoted as slit  $i$  ( $i = 1, 2, 3, 4$ ).<sup>\*</sup>

Star measurements are assumed to be obtained from a spacecraft nominally spinning at a constant rate  $\omega_0$  about a known body axis. Each star mapper has a fixed, known orientation with respect to the spacecraft. Deviations from the nominal spin motion and star mapper geometry

<sup>\*</sup> The development can be generalized to incorporate different slit patterns for each sensor.

are assumed to be small over a spin period. Denoted as  $\delta_{\oplus}$ , these modeling errors are assumed to be independent, normally distributed random variables with zero means and covariance  $P_{\oplus}$ .

Sensor  $j$  is assumed to detect stars of magnitude  $M_{cm}$  or brighter to produce a series of transit time measurements  $t_{ij}^{(k)}$  and visual magnitude measurements  $M_{ij}^{(k)}$  where  $k$  denotes the index of the observed star. The errors in  $t_{ij}^{(k)}$  are assumed to be independent, normally distributed random variables with zero means and covariance  $P_{\tau}$ . The errors in  $M_{ij}^{(k)}$  are assumed to be independent, uniformly distributed random variables with zero means and an error range  $\Delta M$  dependent on  $M_{ij}^{(k)}$ .



### III. COORDINATE SYSTEMS

For the assumed spacecraft motion, it is convenient to specify the orientation of the spacecraft and star mappers in terms of the following coordinate frames:

- Earth-centered inertial reference frames (I frame)
- Spacecraft-centered spin reference frame (O frame)
- Spacecraft-centered body reference frame (B frame)
- Sensor-centered boresight reference frame ( $S_j$  frame)
- Sensor-centered trajectory reference frame ( $N_j$  frame)
- Sensor-centered slit reference frame ( $L_{ij}$  frame)

The spacecraft attitude is specified by the I, O and B frames whose basis vectors are the set of orthogonal unit vectors  $(\hat{x}_I, \hat{y}_I, \hat{z}_I)$ ,  $(\hat{x}_O, \hat{y}_O, \hat{z}_O)$  and  $(\hat{x}_B, \hat{y}_B, \hat{z}_B)$ , respectively. As indicated in Figure 3, the unit vector  $\hat{z}_I$  is directed toward Aries,  $\hat{y}_I$  is along the North Celestial Pole and  $\hat{x}_I$  is in the Celestial Equatorial plane. The unit vector  $\hat{z}_O$  is along the nominal spin direction and  $\hat{x}_O$  and  $\hat{y}_O$  are in the spin plane. The transformation matrix from the I frame to the O frame is denoted as  $C_{O/I}$  and can be expressed as

$$C_{O/I} = [\theta_s]_z [\delta_s]_x [\Omega_s]_y \quad (1)$$

where  $\theta_s$ ,  $\delta_s$  and  $\Omega_s$  denote body attitude angles. The symbols  $[\alpha]_u$ ,  $u = x, y, z$ , represent the following matrices:

$$[\alpha]_x = \begin{bmatrix} 1 & 0 & 0 \\ 0 & \cos \alpha & \sin \alpha \\ 0 & -\sin \alpha & \cos \alpha \end{bmatrix} \quad (2)$$

$$[\alpha]_y = \begin{bmatrix} \cos \alpha & 0 & -\sin \alpha \\ 0 & 1 & 0 \\ \sin \alpha & 0 & \cos \alpha \end{bmatrix} \quad (3)$$

$$[\alpha]_z = \begin{bmatrix} \cos \alpha & \sin \alpha & 0 \\ -\sin \alpha & \cos \alpha & 0 \\ 0 & 0 & 1 \end{bmatrix} \quad (4)$$

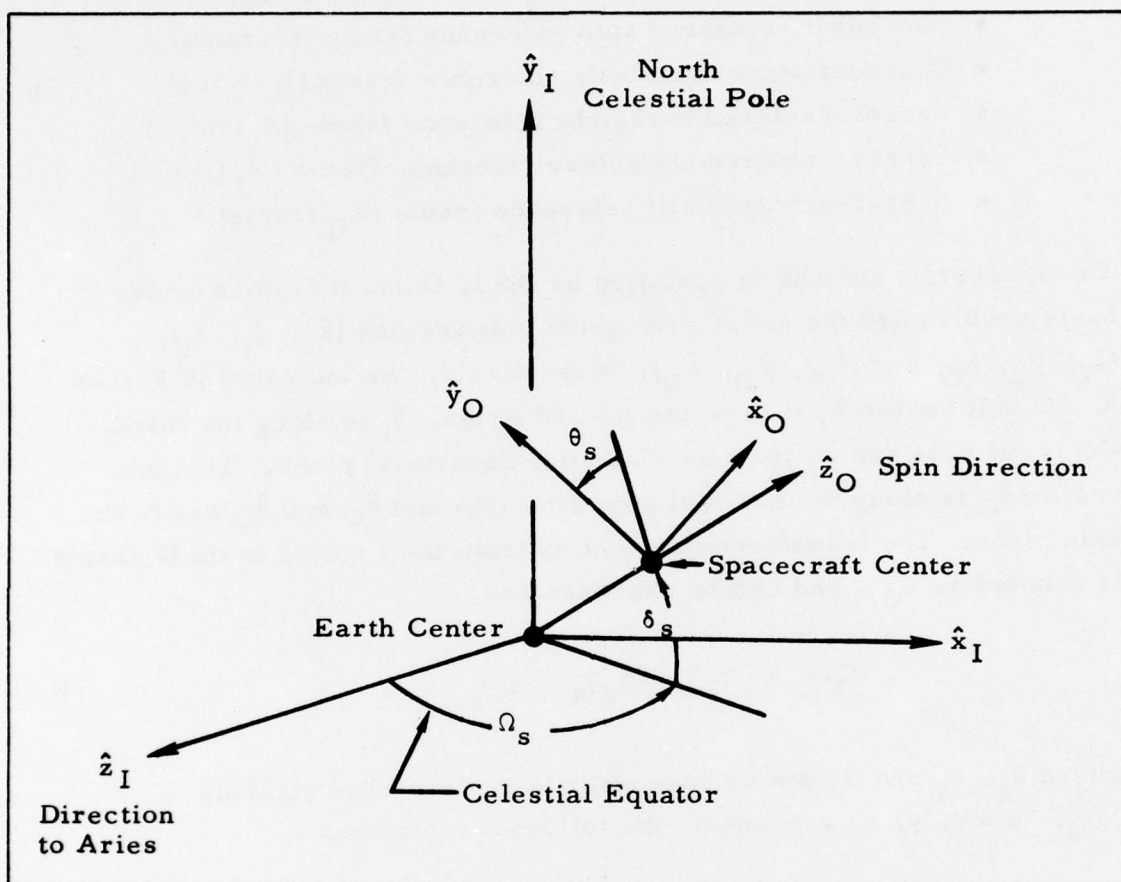


Figure 3. Coordinate System Geometry (I and O Frames)

On the other hand, the O frame is specified relative to the B frame by the transformation matrix  $C_{O/B}$  given as

$$C_{O/B} = [-\delta_B]_x \quad [\Omega_B]_y \quad [\theta_B]_z \quad (5)$$

where  $\delta_B$ ,  $\Omega_B$  and  $\theta_B$  denote known body angles. The above definition allows flexibility in specifying the spin direction relative to the B frame.

It is desirable to describe the orientation of sensor j in terms of two coordinate systems: the  $S_j$  frame and the  $N_j$  frame. The basis vectors of the  $S_j$  and  $N_j$  frames are denoted as  $(\hat{x}_{Sj}, \hat{y}_{Sj}, \hat{z}_{Sj})$  and  $(\hat{x}_{Nj}, \hat{y}_{Nj}, \hat{z}_{Nj})$ , respectively, in which  $\hat{x}_{Sj}$  and  $\hat{x}_{Nj}$  are along the boresight of sensor j and  $\hat{y}_{Sj}, \hat{z}_{Sj}, \hat{y}_{Nj}, \hat{z}_{Nj}$  are in the focal plane of sensor j. The  $S_j$  frame is specified relative to the B frame by the transformation matrix  $C_{Sj/B}$  given as

$$C_{Sj/B} = [-\beta_j]_y [\gamma_j]_z \quad (6)$$

where  $\beta_j$  and  $\gamma_j$  denote boresight angles of sensor j. On the other hand, the  $N_j$  frame is specified relative to the O frame by the transformation matrix  $C_{Nj/O}$  given as

$$C_{Nj/O} = [-E_{bj}]_y [A_{bj}]_z \quad (7)$$

where  $E_{bj}$  and  $A_{bj}$  denote boresight elevation and azimuth angles of sensor j. Since  $\hat{x}_{Sj} = \hat{x}_{Nj}$ , the angles  $E_{bj}$  and  $A_{bj}$  can be related to  $\beta_j, \gamma_j, \delta_B, \Omega_B$  and  $\theta_B$  as

$$E_{bj} = \arcsin(b_{zj}) \quad (8)$$

$$A_{bj} = \arctan(b_{yj}/b_{xj}) \quad (9)$$

where  $b_{xj}, b_{yj}, b_{zj}$  are the O frame components of  $\hat{x}_{Sj}$ , or

$$\begin{bmatrix} b_{xj} \\ b_{yj} \\ b_{zj} \end{bmatrix} = C_{O/B} C_{Sj/B}^T \begin{bmatrix} 1 \\ 0 \\ 0 \end{bmatrix} \quad (10)$$



Moreover, the transformation matrix specifying the  $N_j$  frame relative to the  $S_j$  frame can be expressed as

$$C_{Nj/Sj} = [\rho_j]_x$$

where

$$\rho_j = \arctan \left[ \frac{-\omega_y}{\omega_z} \right] \quad (12)$$

The terms  $\omega_x$ ,  $\omega_y$ ,  $\omega_z$  are the  $S_j$  frame components of the spin direction  $\hat{z}_O$ , or

$$\begin{bmatrix} \omega_x \\ \omega_y \\ \omega_z \end{bmatrix} = C_{O/Sj}^T \begin{bmatrix} 0 \\ 0 \\ 1 \end{bmatrix} \quad (13)$$

The orientation of the slit pattern on sensor  $j$  is specified by the unit vectors  $\hat{x}_{Lij}$ ,  $\hat{y}_{Lij}$ ,  $\hat{z}_{Lij}$  of the  $L_{ij}$  frame, in which  $\hat{y}_{Lij}$  is along slit  $i$ ,  $\hat{x}_{Lij}$  is normal to  $\hat{y}_{Lij}$  in the slit plane and  $\hat{z}_{Lij}$  is normal to the slit plane. As indicated in Figure 4, the  $L_{ij}$  frame is specified relative to the  $S_j$  frame by the transformation matrix  $C_{Lij/Sj}$  given as

$$C_{Lij/Sj} = [\delta_{ij}]_y [\alpha_{ij}]_x \quad (14)$$

where  $\delta_{ij}$  and  $\alpha_{ij}$  denote slit pattern angles of slit  $i$  on sensor  $j$ .

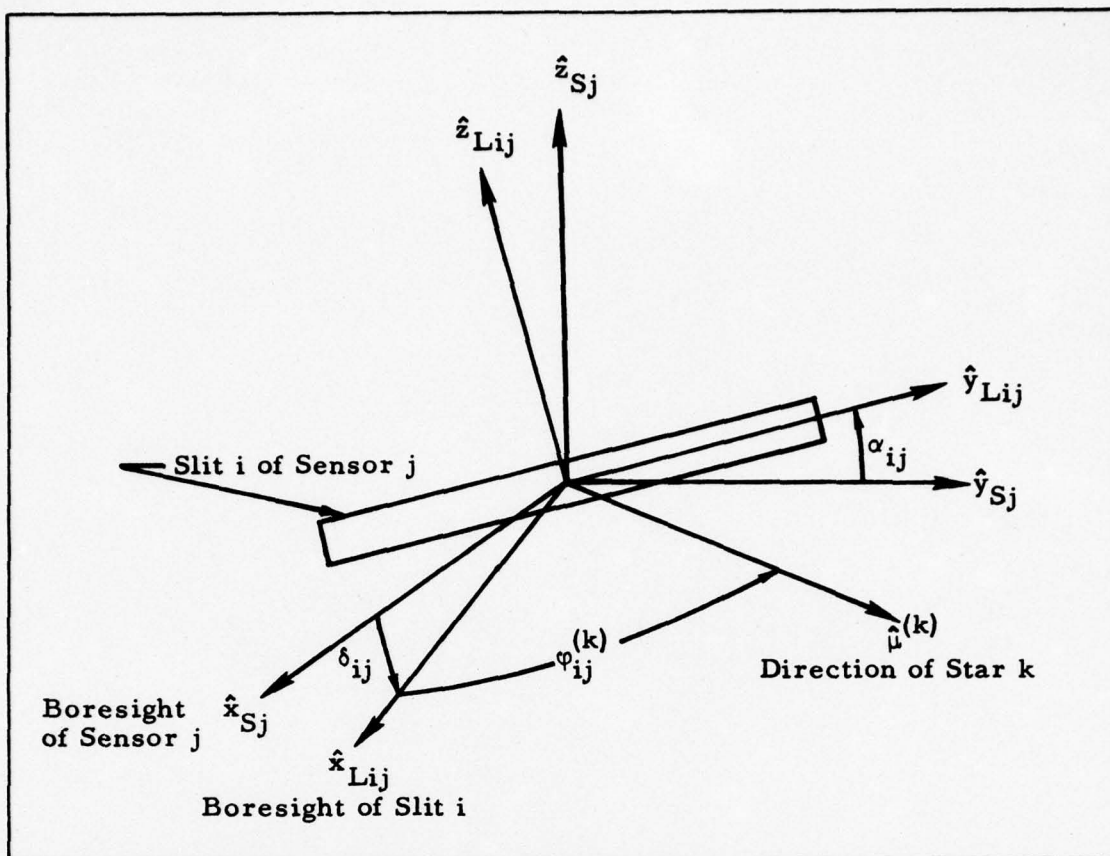


Figure 4. Coordinate System Geometry ( $S_j$  and  $L_{ij}$  Frames)

#### IV. STAR CROSSING GEOMETRY

As the spacecraft spins, the trajectory of a star may cross a number of slits on the star mapper. For the assumed slit pattern, this number ranges from one to four depending on the spin direction and the sensor's orientation relative to the B frame. In particular, there are two basic slit crossing geometries which are of practical interest:\*

Geometry I: 3 Slit Crossings/Star Trajectory

Geometry II: 4 Slit Crossings/Star Trajectory

Loosely speaking, one of the two non-parallel slits is nearly parallel to the  $\hat{y}_{Nj}$  direction in geometry I; none of the slits is oriented along  $\hat{y}_{Nj}$  in geometry II. Since a star trajectory in the  $\hat{y}_{Nj} - \hat{z}_{Nj}$  plane is approximately parallel to  $\hat{y}_{Nj}$ \*\*, the majority of the star trajectories crosses three slits in geometry I and four slits in geometry II.

For a given spin direction, those sensors resulting in geometry I or II are the sensors under consideration in the remaining development. For these sensors, the following transit time difference can be predicted from the star crossing geometry:

$$\Delta t_{Dj} = |t_{3j}^{(k)} - t_{4j}^{(k)}| \quad (15)$$

$$\Delta t_{Ej} = \begin{cases} |t_{2j}^{(k)} - t_{4j}^{(k)}|, & \text{geometry I} \\ |t_{1j}^{(k)} - t_{4j}^{(k)}|, & \text{geometry II} \end{cases} \quad (16)$$

---

\* There is the possibility of a two slit crossing geometry where the two parallel slits are nearly parallel to  $\hat{y}_{Nj}$ . However, this geometry does not permit any means to discriminate between slit crossings above and below the  $\hat{x}_{Nj} - \hat{y}_{Nj}$  plane.

\*\* In actuality, the nominal star trajectory in the  $\hat{y}_{Nj} - \hat{z}_{Nj}$  plane is a curve with mirror symmetry about the  $\hat{z}_{Nj}$  axis.



where  $\Delta t_{Dj}$  denotes the time difference between the parallel slits and  $\Delta t_{Ej}$  denotes the time difference between the extreme parallel and non-parallel slits of a star trajectory. Expressions used to predict  $\Delta t_{Dj}$  and  $\Delta t_{Ej}$  are developed in this section.

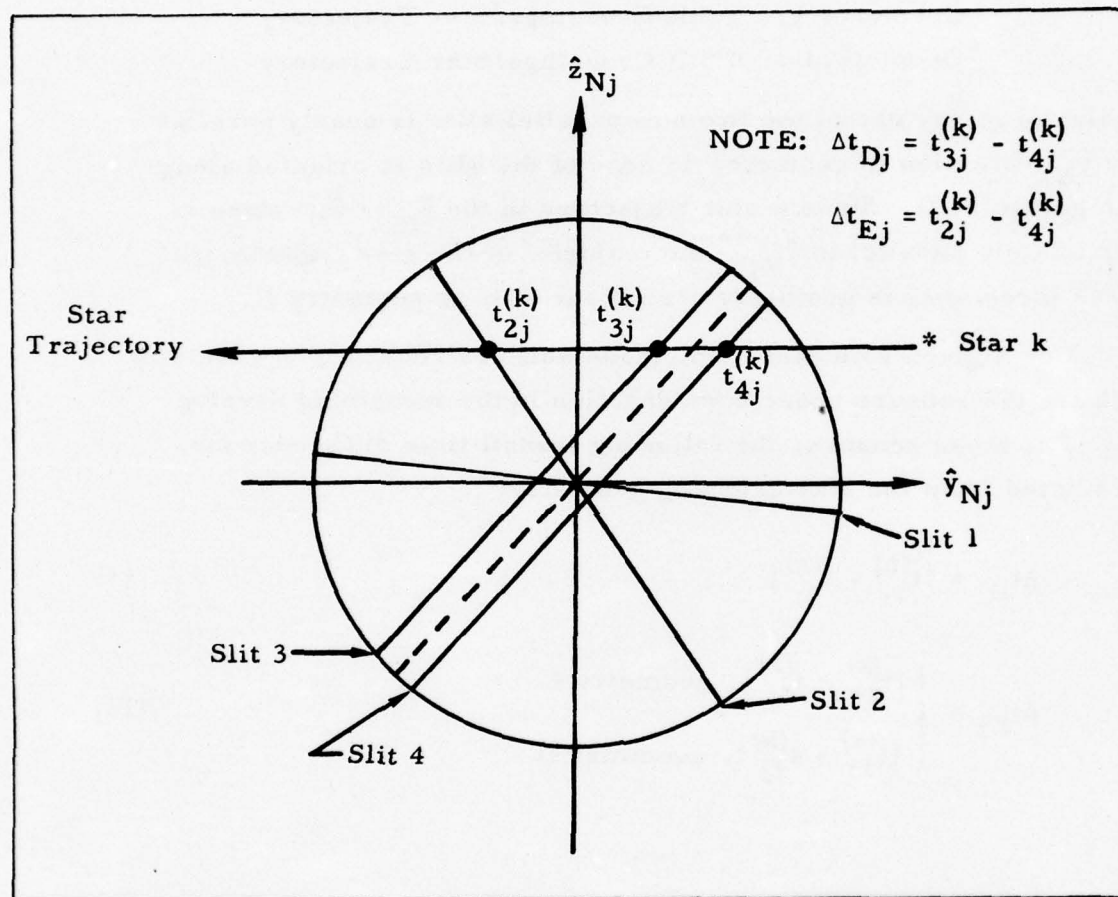


Figure 5. Three Slit Crossing Geometry (Geometry I)

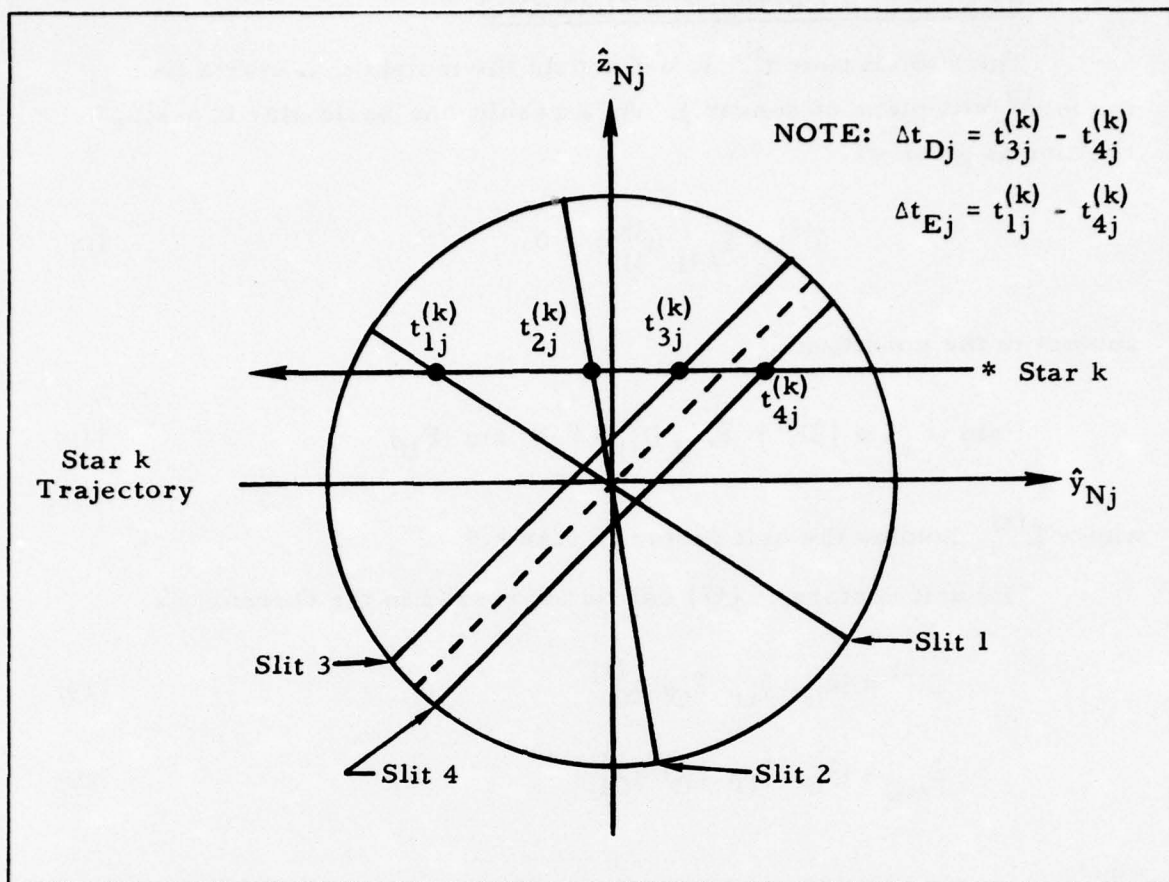


Figure 6. Four Slit Crossing Geometry (Geometry II)

# A. BASIC STAR CROSSING RELATIONS

The transit time  $t_{ij}^{(k)}$  is defined as the instant that star  $k$  lies in the  $i^{\text{th}}$  slit plane of sensor  $j$ . As a result, the basic star crossing relation is given as

$$\hat{\mu}^{(k)} \cdot \hat{z}_{Lij}(t_{ij}^{(k)}) = 0 \quad (17)$$

subject to the condition

$$\sin(F_L) \leq |\hat{\mu}^{(k)} \times \hat{x}_{Lij}(t_{ij}^{(k)})| \leq \sin(F_U) \quad (18)$$

where  $\hat{\mu}^{(k)}$  denotes the unit vector to star  $k$ .\*

The unit vectors of (17) can be expressed in the  $O$  frame as

$$\hat{\mu}^{(k)} = (\hat{x}_O, \hat{y}_O, \hat{z}_O) \mu_O^{(k)} \quad (19)$$

$$\hat{z}_{Lij} = (\hat{x}_O, \hat{y}_O, \hat{z}_O) q_{Oij}^{(k)} \quad (20)$$

where

$$\mu_O^{(k)} = \begin{bmatrix} \cos E_{ij}^{(k)} & \cos A_{ij}^{(k)} \\ \cos E_{ij}^{(k)} & \sin A_{ij}^{(k)} \\ \sin E_{ij}^{(k)} \end{bmatrix} \quad (21)$$

$$q_{Oij}^{(k)} = \begin{bmatrix} q_{xij}^{(k)} \\ q_{yij}^{(k)} \\ q_{zij}^{(k)} \end{bmatrix} \quad (22)$$

---

\* The range of the field-of-view limits,  $F_U$  and  $F_L$ , is between 0 and 90 degrees.



The terms  $E_{ij}^{(k)}$  and  $A_{ij}^{(k)}$  denote elevation and azimuth angles of  $\hat{\mu}^{(k)}$  defined relative to the O frame (see Figure 7). The elements of  $q_{Oij}^{(k)}$  are specified as

$$q_{Oij}^{(k)} = C_{O/B} C_{Sj/B}^T C_{Lij/Sj}^T q_{Lij} \quad (23)$$

where

$$q_{Lij} = \begin{bmatrix} 0 \\ 0 \\ 1 \end{bmatrix} \quad (24)$$

Substituting (19) - (22) into (17) yields

$$q_{xij}^{(k)} \cos E_{ij}^{(k)} \cos A_{ij}^{(k)} + q_{yij}^{(k)} \cos E_{ij}^{(k)} \sin A_{ij}^{(k)} + q_{zij}^{(k)} \sin E_{ij}^{(k)} = 0 \quad (25)$$

Through the relations of (5), (6) and (14), it is seen that (25) involves  $E_{ij}^{(k)}$ ,  $A_{ij}^{(k)}$ ,  $\delta_B$ ,  $\Omega_B$ ,  $\theta_B$ ,  $\beta_j$ ,  $\gamma_j$ ,  $\delta_{ij}$  and  $\alpha_{ij}$ . Among these parameters,  $\delta_B$ ,  $\Omega_B$ ,  $\theta_B$ ,  $\beta_j$  and  $\gamma_j$  are known and  $E_{ij}^{(k)}$ ,  $A_{ij}^{(k)}$ ,  $\delta_{ij}$  and  $\alpha_{ij}$  are unknown.

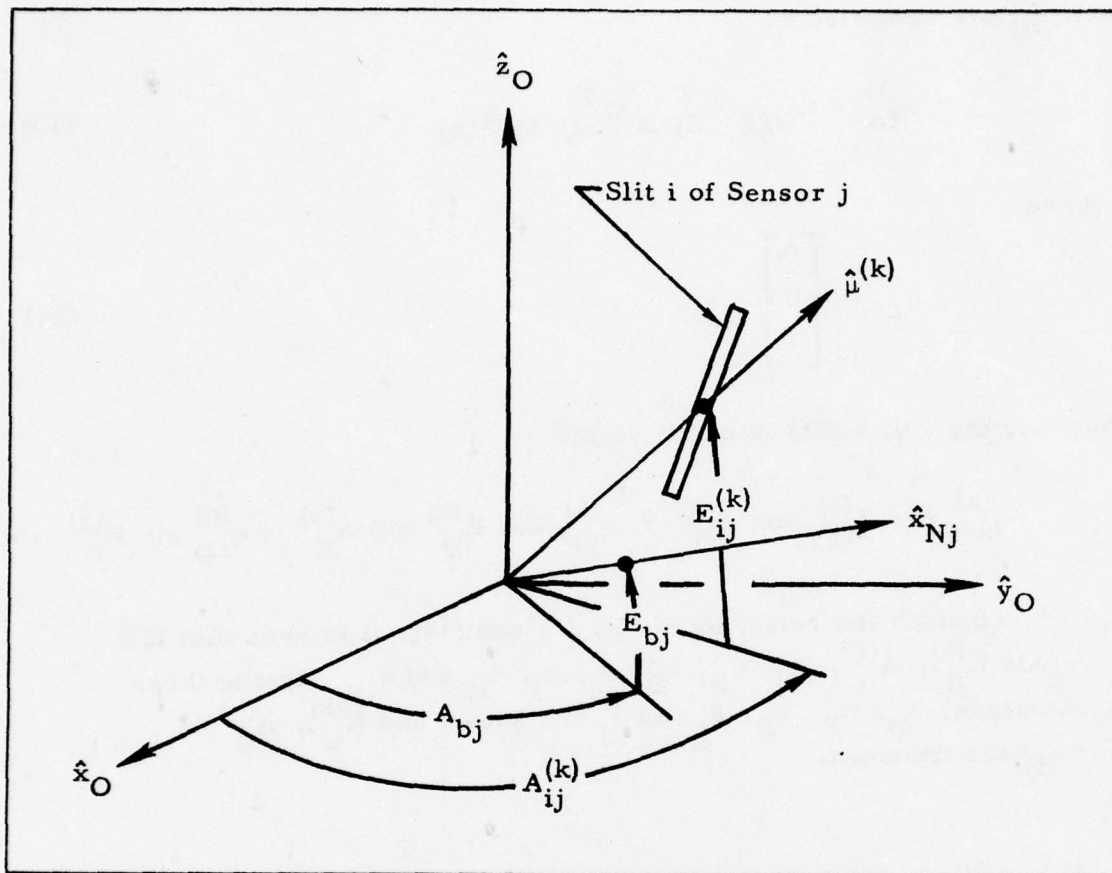


Figure 7. Star Crossing Geometry

## B. SLIT RELATIONS

In general, the elevation and azimuth terms in (25) can be expressed as

$$E_{ij}^{(k)} = E_{bj} + \eta_{ij}^{(k)} \quad (26)$$

$$A_{ij}^{(k)} = A_{bj} + \Delta_{ij}^{(k)} \quad (27)$$

where  $\eta_{ij}^{(k)}$  denotes the elevation of  $\hat{\mu}^{(k)}$  relative to the  $\hat{x}_{Nj} - \hat{y}_{Nj}$  plane and  $\Delta_{ij}^{(k)}$  denotes the azimuth angle defined relative to  $A_{bj}$  in the  $\hat{x}_O - \hat{y}_O$  plane. Also it is noted that

$$q_O^{(ij)} = C_{Nj/O}^T C_{Nj/Sj} C_{Lij/Sj}^T q_{Lij} \quad (28)$$

Substituting (26) - (28) into (25) yields

$$\begin{aligned} d_{xi} \cos(E_{bj} + \eta_{ij}^{(k)}) \cos \Delta_{ij}^{(k)} + d_{yi} \cos(E_{bj} + \eta_{ij}^{(k)}) \sin \Delta_{ij}^{(k)} \\ + d_{zi} \sin(E_{bj} + \eta_{ij}^{(k)}) = 0 \end{aligned} \quad (29)$$

where

$$d_{xi} = \cos E_{bj} \sin \delta_{ij} - \sin E_{bj} \cos \psi_{ij} \cos \delta_{ij} \quad (30)$$

$$d_{yi} = -\sin \psi_{ij} \cos \delta_{ij} \quad (31)$$

$$d_{zi} = \sin E_{bj} \sin \delta_{ij} + \cos E_{bj} \cos \psi_{ij} \cos \delta_{ij} \quad (32)$$

$$\psi_{ij} = \alpha_{ij} - \rho_j \quad (33)$$



Furthermore,  $\eta_{ij}^{(k)}$  can be expressed as

$$\eta_{ij}^{(k)} = \arcsin [\sin \psi_{ij} \sin \varphi_{ij}^{(k)} - \cos \psi_{ij} \sin \delta_{ij} \cos \varphi_{ij}^{(k)}] \quad (34)$$

where the terms  $\varphi_{ij}^{(k)}$  denotes the angle between  $\hat{\mu}^{(k)}$  and  $\hat{x}_{Lij}$ .

Suppose star  $k$  crossed slit  $i$  at time  $t_{ij}^{(k)}$  and slit  $i'$  at time  $t_{i'j}^{(k)}$ . The predicted time difference between  $t_{i'j}^{(k)}$  and  $t_{ij}^{(k)}$  can be expressed as

$$\Delta t_{i'/i}^{(k)} = \frac{\Delta_{i'j}^{(k)} - \Delta_{ij}^{(k)}}{\omega_0} \quad (35)$$

Given slit  $i$  and  $\varphi_{ij}^{(k)}$ , one can first determine  $\eta_{ij}^{(k)}$  using (34) and then numerically solve (29) for  $\Delta_{ij}^{(k)}$ . Similarly with  $i = i'$ , one can numerically solve (29) for  $\Delta_{i'j}^{(k)}$  under the constraint  $\eta_{i'j}^{(k)} = \eta_{ij}^{(k)}$  and subsequently determine  $\Delta t_{i'/i}^{(k)}$  using (35).

Because  $\varphi_{ij}^{(k)}$  or  $\eta_{ij}^{(k)}$  is not known, the predicted time differences for  $\Delta t_{Dj}$  and  $\Delta t_{Ej}$  are approximated. In particular, the time  $\Delta t_{Dj}$  between the parallel slits is predicted from (35) under the condition

$$\eta_{i'j}^{(k)} = \eta_{ij}^{(k)} = 0 \quad (i', i = 3, 4) \quad (36)$$

The resulting value of  $\Delta t_{Dj}$  represents an average over the field of view limits.

The time  $\Delta t_{Ej}$  between the extreme slits is predicted from (35) under the condition

$$\varphi_{ij}^{(k)} = -F_U \operatorname{sgn}(E_{bj}) \quad (37)$$

$$\eta_{i'j}^{(k)} = \eta_{ij}^{(k)} \quad (38)$$

where

$$i', i = \begin{cases} 2, 4 & ; \text{ geometry I} \\ 1, 4 & ; \text{ geometry II} \end{cases} \quad (39)$$

and  $\text{sgn}(x)$  denotes the sign of  $x$ . Thus  $\Delta t_{Dj}$  and  $\Delta t_{Ej}$  can be predicted directly from the star crossing geometry.

### C. ARC LENGTH RELATIONS

Given knowledge of the slits, it is possible to specify the star's direction in the O frame. To this end, it is assumed that  $t_{ij}^{(k)}$  and  $t_{i'j}^{(k)}$  are two transit times resulting from star k crossing slits i and i' on sensor j (i, i' ≠ 3, 4). In this case, the elevation and azimuth angles at these two times are related as

$$E_{i'j}^{(k)} = E_{ij}^{(k)} \quad (40)$$

$$A_{i'j}^{(k)} = A_{ij}^{(k)} - \theta_{i'i}^{(k)} \quad (41)$$

where

$$\theta_{i'i}^{(k)} = \omega_o (t_{ij}^{(k)} - t_{i'j}^{(k)}) \quad (42)$$

and  $t_{ij}^{(k)} < t_{i'j}^{(k)}$ .

The star crossing conditions for the two times are represented by two equations in the form of (25). Solving these equations simultaneously with (40) and (41) yields

$$A_{ij}^{(k)} = \arctan \left[ \frac{q_i^{(k)} T \quad N_A^{(k)} \quad q_{i'}^{(k)}}{q_i^{(k)} T \quad D_A^{(k)} \quad q_{i'}^{(k)}} \right] \quad (43)$$

$$E_{ij}^{(k)} = \arctan \left[ \frac{N_E^{(k)} \quad q_i^{(k)}}{D_E^{(k)} \quad q_i^{(k)}} \right] \quad (44)$$

where

$$q_i^{(k)} = q_{Oij}^{(k)} \quad (45)$$



$$q_{i'i}^{(k)} = q_{O i'j}^{(k)} \quad (46)$$

$$N_A^{(k)} = \begin{bmatrix} 0 & 0 & 1 \\ 0 & 0 & 0 \\ -\cos \theta_{i'i}^{(k)} & \sin \theta_{i'i}^{(k)} & 0 \end{bmatrix} \quad (47)$$

$$D_A^{(k)} = \begin{bmatrix} 0 & 0 & 0 \\ 0 & 0 & -1 \\ \sin \theta_{i'i}^{(k)} & \cos \theta_{i'i}^{(k)} & 0 \end{bmatrix} \quad (48)$$

A similar group of expressions can be obtained at times  $t_{ij}^{(\ell)}$  and  $t_{i'j}^{(\ell)}$  which corresponds to star  $\ell$ . To be specific, the terms  $E_{ij}^{(\ell)}$ ,  $E_{i'j}^{(\ell)}$ ,  $A_{ij}^{(\ell)}$  and  $A_{i'j}^{(\ell)}$  are described by (40) - (48) with  $\ell$  substituted for  $k$ .

The arc length between stars  $k$  and  $\ell$  is defined as

$$\widehat{d}_{k\ell} = \arccos \left[ \hat{\mu}^{(k)} \cdot \hat{\mu}^{(\ell)} \right] \quad (49)$$

The O frame components of  $\hat{\mu}^{(k)}$  at time  $t_{ij}^{(k)}$  and  $\hat{\mu}^{(\ell)}$  at time  $t_{ij}^{(\ell)}$  have the form of (19). Substituting these components into (49) yields

$$\begin{aligned} \widehat{d}_{k\ell} = \arccos \left\{ \sin E_{ij}^{(k)} \sin E_{ij}^{(\ell)} \right. \\ \left. + \cos E_{ij}^{(k)} \cos E_{ij}^{(\ell)} \cos \left[ A_{ij}^{(k)} - A_{ij}^{(\ell)} + \omega_O (t_{ij}^{(k)} - t_{ij}^{(\ell)}) \right] \right\} \quad (50) \end{aligned}$$

Thus  $\widehat{d}_{k\ell}$  is expressed in terms of the transit times  $t_{ij}^{(k)}$ ,  $t_{i'j}^{(k)}$ ,  $t_{ij}^{(\ell)}$  and  $t_{i'j}^{(\ell)}$ . In contrast, the arc length of stars  $\alpha$  and  $\beta$  from a star catalog is expressed as

---

\* Equation (50) is readily extended to the situation where the transits result from two different sensors.

$$\widehat{d}_{\alpha\beta} = \arccos \left\{ \sin \delta_{\alpha} \sin \delta_{\beta} + \cos \delta_{\alpha} \cos \delta_{\beta} \cos (\Omega_{\alpha} - \Omega_{\beta}) \right\} \quad (51)$$

where  $(\delta_{\alpha}, \Omega_{\alpha})$  and  $(\delta_{\beta}, \Omega_{\beta})$  denote the declination and right ascension angles of stars  $\alpha$  and  $\beta$ , respectively.

#### D. ERROR RELATIONS

The previous sections indicate that  $\Delta t_{Dj}$  and  $\widehat{d}_{kl}$  can be expressed as

$$\Delta t_{Dj} = \Delta t_{Dj} (\Theta, \eta) \quad (52)$$

$$\widehat{d}_{kl} = \widehat{d}_{kl} (\Theta, \tau) \quad (53)$$

where

$$\Theta = [\delta_{ij}, \delta_{i'j}, \alpha_{ij}, \alpha_{i'j}, \beta_j, \gamma_j, \delta_\beta, \Omega_\beta, \theta_\beta]^T \quad (54)$$

$$\eta = [\eta_{ij}^{(k)}, \eta_{i'j}^{(k)}]^T \quad (55)$$

$$\tau = [t_{ij}^{(k)}, t_{i'j}^{(k)}, t_{ij}^{(\ell)}, t_{i'j}^{(\ell)}] \quad (56)$$

If  $\Theta_N$  and  $\eta_N$  denotes the nominal values of  $\Theta$  and  $\eta$ , respectively, deviations about the nominal can be expressed as

$$\delta\Theta = \Theta - \Theta_N \quad (57)$$

$$\delta\eta = \eta - \eta_N \quad (59)$$

where

$$\eta_N = [0, 0]^T \quad (59)$$

The terms  $\delta\Theta$  and  $\delta\eta$  represent system model errors. Measured transit times are represented by  $\tau$  and their errors are denoted as  $\delta\tau$ .

To approximate the effects of model and measurement errors on  $\Delta t_{Dj}$  and  $\widehat{d}_{kl}$ , (52) and (53) are linearized about  $\Theta_N$ ,  $\eta_N$  and  $\tau$  to yield

$$\Delta t_{Dj} = J_{t\Theta} \delta\Theta + J_{t\eta} \delta\eta \quad (60)$$

$$\widehat{d}_{kl} = J_{d\Theta} \delta\Theta + J_{d\tau} \delta\tau \quad (61)$$



where

$$J_{t\Theta} = \frac{\partial \Delta t_{Dj}}{\partial \Theta} \bigg|_{\Theta_N, \eta_N} \quad (62)$$

$$J_{t\eta} = \frac{\partial \Delta t_{Dj}}{\partial \eta} \bigg|_{\Theta_N, \eta_N} \quad (63)$$

$$J_{d\Theta} = \frac{\partial \widehat{d}_{kl}}{\partial \Theta} \bigg|_{\Theta_N, \tau} \quad (64)$$

$$J_{d\tau} = \frac{\partial \widehat{d}_{kl}}{\partial \tau} \bigg|_{\Theta_N, \tau} \quad (65)$$

In this development,  $\delta\Theta$ ,  $\delta\eta$  and  $\delta\tau$  are assumed to be normally distributed random variables with zero means and the following second-order statistics:

$$E [\delta\Theta \delta\Theta^T] = P_{\Theta} \quad (66)$$

$$E [\delta\eta \delta\eta^T] = P_{\eta} \quad (67)$$

$$E [\delta\tau \delta\tau^T] = P_{\tau} \quad (68)$$

$$E [\delta\eta \delta\Theta^T] = 0 \quad (69)$$

$$E [\delta\eta \delta\tau^T] = 0 \quad (70)$$

$$E [\delta\tau \delta\Theta^T] = 0 \quad (71)$$

where  $P_{\Theta}$ ,  $P_{\tau}$  and  $P_{\eta}$  denote covariance matrices of  $\delta\Theta$ ,  $\delta\tau$  and  $\delta\eta$ , respectively. The error covariances  $P_{\Theta}$  and  $P_{\tau}$  are specified by the problem at hand. The error covariance  $P_{\eta}$  can be modeled as

$$P_{\eta} = \sigma_{\eta}^2 I_{2 \times 2} \quad (72)$$

when

$$\sigma_{\eta} = \text{MAX}_{i, i'} [\eta_{ij}(F_U), \eta_{i'j}(F_U)] \quad (73)$$

The terms  $\eta_{ij}$  and  $\eta_{i'j}$  are computed from (34) with  $\phi_{ij} = \phi_{i'j} = F_U$ ;  $I_{n \times n}$  is an  $n \times n$  identity matrix.

Based on the first-order approximations of (60) - (61) and the statistics of (66) - (71),  $\Delta_{Dj}$  and  $\bar{d}_{kl}$  become normally distributed with zero means and variances  $\sigma_{tD}^2$  and  $\sigma_{kl}^2$ , respectively, where

$$\sigma_{tD}^2 = J_{t\Theta} P_{\Theta} J_{\Theta}^T + J_{t\eta} P_{\eta} J_{t\eta}^T \quad (74)$$

$$\sigma_{kl}^2 = J_{d\Theta} P_{\Theta} J_{d\Theta}^T + J_{d\tau} P_{\tau} J_{d\tau}^T \quad (75)$$

## V. STAR IDENTIFICATION

The approach to star identification begins with a set of star measurements obtained from a spinning spacecraft. In this case, the relative times between successive slit crossings are predicted from the star crossing geometry. These predictions are compared to transit time data to provide a basis for slit identification. Those data matching the time predictions and having similar visual magnitudes are designated as "multiple" transit data. The remaining data are designated as "single" transit data.

Once the slits are identified, the arc lengths between stars are computed from the multiple transit data and compared to those from a star catalog. Among the star-pair combinations matching the data, a selection is made on those stars that form a consistent star-pair chain.

A flow chart of the star identification method is shown in Figure 8. It is noted that the method consists of three basic operations: (1) an initialization operation which inputs measurement and model data and computes system parameters, (2) a screen operation which identifies and isolates multiple transit data and (3) a star selection operation which identifies stars corresponding to the multiple transit data.

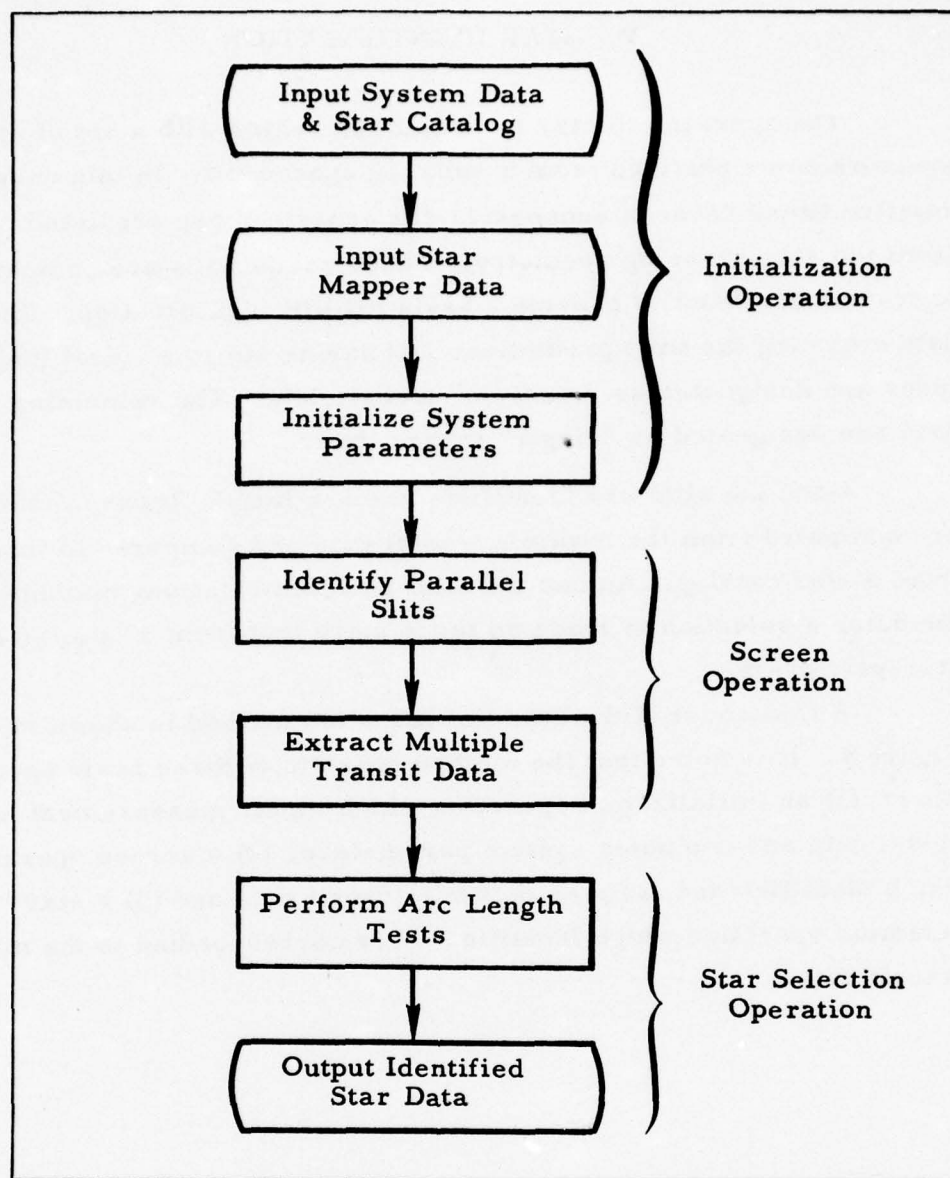


Figure 8. Flow Chart of the Basic Star Identification Operations



#### A. INITIALIZATION

The first task is to input system data, a star catalog and star mapper data. System data include star mapper geometry parameters ( $\gamma_j, \beta_j, \alpha_{ij}, \delta_{ij}, F_U, F_L$ ), spin motion parameters ( $\omega_o, \delta_\beta, \Omega_\beta, \theta_\beta$ ), and error parameters ( $P_\theta, P_\tau, \Delta M$ ). The star catalog consists of line of sight parameters ( $\delta_\alpha, \Omega_\alpha$ ) and the cataloged visual magnitude ( $M_c^{(\alpha)}$ ) associated with star  $\alpha$ . Once obtained, the star catalog is reduced by accounting for the maximum sensitivity of the star mappers, (i.e.,  $M_{ij}^{(k)} \leq M_{cm}$ ), any a priori knowledge of the inertial spin direction, and the effects of star obscuration (e.g., by the Earth). The reduction results in a limited star catalog which is used for the star selection task.

The star mapper data consists of a series of transit times and visual magnitudes ( $t_{ij}^{(k)}, M_{ij}^{(k)}$ ). For this discussion, it is assumed that the raw data have been processed over a number of spin periods (scans) to reduce the amount of spurious transits. To this end, multi-scan techniques can be used if the spacecraft does not appreciably precess during successive scans.<sup>(3)</sup> Once completed, the resulting data are reduced to a single scan for star identification.

## B. SCREEN OPERATION

The screen operation consists of a series of tests to isolate and identify multiple transit data. The first test is aimed at isolating those pairs of transits associated with a star crossing the parallel slits (i.e., slits 3 and 4). If two transits are from the same sensor and within a field-of-view time window, then they qualify as a candidate pair. Given a candidate pair with transit times  $t_{lj}$  and  $t_{mj}$  and magnitudes  $M_{lj}$  and  $M_{mj}$  from sensor  $j$ , a time residual  $r_{Dj}$  and a magnitude residual  $r_{Mj}$  are computed as follows:

$$r_{Dj} = t_{mj} - t_{lj} - \Delta t_{Dj} \quad (76)$$

$$r_{Mj} = M_{mj} - M_{lj} \quad (77)$$

where  $\Delta t_{Dj}$  is specified by (35) and (36). Also a time score  $C_{Dj}$  and a magnitude score  $C_{Mj}$  are computed as

$$C_{Dj} = r_{Dj}^2 V_t^{-1} \quad (78)$$

$$C_{Mj} = |r_{Mj}| \quad (79)$$

where

$$V_t = 2 \sigma_t^2 + \sigma_{tD}^2 \quad (80)$$

The term  $\sigma_t^2$  is a specified variance of the transit time measurement error and  $\sigma_{tD}^2$  is computed from (74).

The decision rule is to accept the times ( $t_{lj}$ ,  $t_{mj}$ ) as "double slit" times if the following inequalities are true:

$$C_{Dj} < C_{DB} \quad (81)$$

$$C_M < \Delta M$$

(82)

where  $C_{DB}$  is a threshold level for the double slit test. Because of the assumptions on the error statistics, the residuals  $r_{Dj}$  is normally distributed. Thus the score  $C_{Dj}$  has a chi-squared distribution with one degree of freedom. Moreover, given a specified probability of a correct decision, the threshold  $C_{DB}$  can be obtained from standard tables. (4)

The next task is to isolate the remaining transits associated with the double slit transits. To this end,  $\Delta t_{Ej}$  is computed from (35) and (37) - (39) to provide a time window. Transit times are checked on both sides of the double slit times to determine if they are within the window. Those candidates within the window are tested for similar visual magnitudes as in the double slit test. Furthermore, the number of candidates within the window are checked for consistency with the known star crossing geometry. The allowable number of candidates/windows is one in geometry I and two in geometry II. If there is an allowable number on both sides of the double transits, both candidates are rejected to avoid ambiguity.

Those candidates with the allowable number are combined with the double transits to form the  $k^{th}$  multiple transit group. Slit designations are assigned and the parameters  $A_{ij}^{(k)}$  and  $E_{ij}^{(k)}$  are computed via (43) - (48). The above process continues until all of the transits have been considered.

### C. STAR SELECTION OPERATION

The star selection operation consists of an arc length test, a star-pair consistency test and a magnitude test.

The arc length test begins by computing the arc length between two stars associated with the first two multiple transit groups. In general, for groups  $k$  and  $l$  ( $k \neq l$ ), the arc length  $\widehat{d}_{kl}$  is computed via (50). Then a residual  $r_{kl}^{\alpha\beta}$  is computed from  $\widehat{d}_{kl}$  and the arc length  $\widehat{d}_{\alpha\beta}$  between stars  $\alpha$  and  $\beta$  of the limited star catalog as

$$r_{kl}^{\alpha\beta} = \widehat{d}_{\alpha\beta} - \widehat{d}_{kl} \quad (83)$$

where  $\widehat{d}_{\alpha\beta}$  is specified in (51). Furthermore, a chi-squared score  $C_{kl}^{\alpha\beta}$  based on the residual is computed as

$$C_{kl}^{\alpha\beta} = (r_{kl}^{\alpha\beta})^2 / \sigma_{kl}^2 \quad (84)$$

where  $\sigma_{kl}^2$  is specified in (75).

The decision rule is to accept the stars  $\alpha$  and  $\beta$  as candidates if

$$C_{kl}^{\alpha\beta} < C_{AB} \quad (85)$$

where  $C_{AB}$  is a threshold selected to meet a specified probability of correct decision; otherwise, the star-pair is rejected. Every star-pair combination in the limited catalog is tested in this manner.

Once the star candidates for groups  $(k, l)$  are obtained, the same procedure is used to obtain candidates for groups  $(l, m)$  and  $(k, m)$ . Given star candidates for three groups of data, a search is conducted to identify those candidates which are logically consistent with the data. For example, stars  $\alpha$ ,  $\beta$  and  $\gamma$  comprise a consistent triplet if each is a candidate in only two of the groups  $(k, l)$ ,  $(l, m)$  and  $(k, m)$ .



Finally, each of the candidates comprising a consistent triplet is subjected to a magnitude test. In this case, a residual  $r_{Mk}^{\alpha}$  is computed from the cataloged visual magnitude  $M_c^{(\alpha)}$  of star  $\alpha$  and the average magnitude associated with the  $k^{\text{th}}$  multiple transit group, or

$$r_{Mk}^{\alpha} = M_c^{(\alpha)} - \overline{M}^{(k)} \quad (86)$$

where

$$\overline{M}^{(k)} = \sum_{i=1}^{n_k} M_{ij}^{(k)} / n_k \quad (87)$$

and  $n_k$  denotes the total number of transits for the  $k^{\text{th}}$  group. The rule is to accept the three candidates as stars associated with the multiple transit group  $k$  if all three stars satisfy

$$|r_{Mk}^{\alpha}| < \Delta M \quad (88)$$

In a similar manner, star triplets are identified for the next three transit groups (i.e., the last two of the previous group and one additional set). The process continues until all of the transit groups are considered. Each candidate star is thus required to form a consistent triplet with three other pairs of candidates--the preceding pair, the subsequent pair, and the pair just before and after the candidate.

## VI. ATTITUDE DETERMINATION

The problem is to determine an estimate of the spacecraft's inertial attitude based on star mapper measurements. It is noted that the transformation matrix between the B and I frames can be expressed as

$$C_{B/I} = C_{O/B}^T (\theta_B, \Omega_B, \delta_B) C_{O/I} (\theta_s, \Omega_s, \delta_s) \quad (89)$$

Assuming that  $\theta_B$ ,  $\Omega_B$  and  $\delta_B$  of  $C_{O/B}$  are known, the problem is reduced to determining  $\delta_s$ ,  $\Omega_s$  and  $\theta_s$ .

A gross estimate can be obtained by utilizing line of sight information of stars identified with the multiple transit data. Specifically, the inertial components of  $\hat{\mu}^{(\alpha)}$  can be expressed as

$$\mu_I^{(\alpha)} = C_{O/I}^T (\delta_s, \Omega_s, \theta_s) \mu_O^{(\alpha)} \quad (90)$$

where

$$\mu_I^{(\alpha)} = \begin{bmatrix} \cos \delta_\alpha \sin \Omega_\alpha \\ \sin \Omega_\alpha \\ \cos \delta_\alpha \cos \Omega_\alpha \end{bmatrix} \quad (91)$$

and  $\mu_O^{(\alpha)}$  is specified in (21) in terms of  $A_{ij}^{(\alpha)}$  and  $E_{ij}^{(\alpha)}$  which are known for each multiple transit group. Thus (90) provides two independent relations for each identified star.

The undetermined parameters  $\delta_s$ ,  $\Omega_s$  and  $\theta_s$  can be estimated based on the following model:

$$\delta_s(t) = \delta_{s0} \quad (92)$$

$$\Omega_s(t) = \Omega_{s0} \quad (93)$$

$$\theta_s(t) = \omega_o(t - t_o) + \theta_{s0} \quad (94)$$

where  $\delta_{so}$ ,  $\Omega_{so}$  and  $\theta_{so}$  are constants corresponding to time  $t_o$ .

Thus given  $N$  identified stars, the estimation problem can be formulated to select parameters  $\delta_{so}$ ,  $\Omega_{so}$  and  $\theta_{so}$  such that they minimize the estimation error

$$e = \sum_{m=1}^3 (p_m - \hat{p}_m)^2 \quad (95)$$

subject to the constraints of (90) - (94) and

$$\begin{bmatrix} p_1 \\ p_2 \\ p_3 \end{bmatrix} = \begin{bmatrix} \delta_{so} \\ \Omega_{so} \\ \theta_{so} \end{bmatrix} \quad (96)$$

The term  $\hat{p}_m$  denotes the estimate of  $p_m$  where  $m = 1, 2, 3$ . Given at least two identified stars, the estimates can be computed via an iterative least-squares procedure. Once  $\hat{p}_m$  are known, estimates of  $\delta_s$ ,  $\Omega_s$  and  $\theta_s$  are computed as

$$\hat{\delta}_s = \hat{\delta}_{so} \quad (97)$$

$$\hat{\Omega}_s = \hat{\Omega}_{so} \quad (98)$$

$$\hat{\theta}_s = \omega_o (t - t_o) + \hat{\theta}_{so} \quad (99)$$

Finally, the estimate of the spacecraft's inertial attitude is represented by the matrix

$$\hat{C}_{B/I} = C_{O/B}^T C_{O/I} (\hat{\theta}_s, \hat{\Omega}_s, \hat{\delta}_s) \quad (100)$$

A reasonably close initial estimate of the unknown parameters can be obtained from the data of two identified stars. Given  $\mu_O^{(\alpha)}$ ,  $\mu_O^{(\beta)}$ ,  $\mu_I^{(\alpha)}$  and  $\mu_I^{(\beta)}$  of stars  $\alpha$  and  $\beta$ , the unknown parameters  $p_1$  and  $p_2$  can be computed as follows:

$$p_1 = \arcsin(s_{Iy}) \quad (101)$$

$$p_2 = \arctan(s_{Ix}/s_{Iz}) \quad (102)$$

where  $s_{Ix}$ ,  $s_{Iy}$ ,  $s_{Iz}$  are the I-frame components of the spin direction, or

$$s_I = (s_{Ix}, s_{Iy}, s_{Iz})^T \quad (103)$$

But  $s_I$  can be expressed as

$$s_I = A_I A_{SI}^{-1} s_{SI} \quad (104)$$

where

$$s_{SI} = (0, 0, 1)^T \quad (105)$$

$$A_{SI} = [\mu_{SI}^{(\alpha)} \quad \mu_{SI}^{(\beta)} \quad n_{SI}^{(\alpha\beta)}]_{3 \times 3} \quad (106)$$

$$A_I = [\mu_I^{(\alpha)} \quad \mu_I^{(\beta)} \quad n_I^{(\alpha\beta)}]_{3 \times 3} \quad (107)$$

$$\mu_{SI}^{(\alpha)} = [\omega_O (t_{ij}^{(\alpha)} - t_O) + \theta_{so}]_z^T \mu_O^{(\alpha)} \quad (108)$$

$$\mu_{SI}^{(\beta)} = [\omega_O (t_{ij}^{(\beta)} - t_O) + \theta_{so}]_z^T \mu_O^{(\beta)} \quad (109)$$

The terms  $n_{SI}^{(\alpha\beta)}$  and  $n_I^{(\alpha\beta)}$  are inertial components of the vector  $\hat{n}^{(\alpha\beta)}$  which is orthogonal to  $\hat{\mu}^{(\alpha)}$  and  $\hat{\mu}^{(\beta)}$ , or



$$\hat{n}^{(\alpha\beta)} = \frac{\hat{\mu}^{(\alpha)} \times \hat{\mu}^{(\beta)}}{|\hat{\mu}^{(\alpha)} \times \hat{\mu}^{(\beta)}|} \quad (110)$$

Thus for a given  $\theta_{so}$ , the elements of  $\mu_{SI}^{(\alpha)}$  and  $\mu_{SI}^{(\beta)}$  and hence  $p_1$  and  $p_2$  can be computed. In turn, an estimate of  $p_3$  can be determined as

$$p_3 = \arctan \left\{ \frac{\sin p_1 \sin p_2 \mu_{Ix}^{(\alpha)} + \cos p_1 \mu_{Iy}^{(\alpha)} + \sin p_1 \cos p_2 \mu_{Iz}^{(\alpha)}}{\cos p_2 \mu_{Ix} - \sin p_2 \mu_{Iz}} \right\}$$

$$-A_{ij}^{(\alpha)} - \omega_o (t_{ij}^{(\alpha)} - t_o) \quad (111)$$

Once an attitude estimate is obtained, a detailed star identification operation can begin. A typical procedure is to predict transit times based on the gross attitude estimate and to match the results with the measured single transit data.<sup>(3)</sup>

## VII. NUMERICAL STUDY

A brief numerical study was conducted to test the feasibility of the proposed star identification method. To this end, a computer program with the basic operations was implemented and tested with simulated star data. The tests consisted of generating star mapper data under known conditions and then processing the data through the program to identify stars and estimate spacecraft attitude. A measure of performance was obtained by comparing the program's results to the true star observations and attitude motion.

#### A. RUN CONDITIONS

Star data were generated for two basic types of spacecraft motion: (1) pure spin motion (designated as motion A) and (2) nutation motion (designated as motion B). In motion A, the spin rate was set to  $\omega_o + \Delta\omega_o$ , where  $\Delta\omega_o$  denotes a spin rate error assumed as

$$\frac{\Delta\omega_o}{\omega_o} = 2\pi \times 10^{-4} \quad (112)$$

Thus the actual spin angle was simulated as

$$\theta_s = \theta_{so} + (\omega_o + \Delta\omega_o) (t - t_o) \quad (113)$$

In motion B, spacecraft was assumed to cone and precess away from the nominal spin direction. In particular, the half-cone angle was set to  $|\delta_{3j}|$  and the cone frequency was  $2\omega_o$ ; the precession rate was  $2 \times 10^{-4} \omega_o$ .

Three star mappers were assumed to be oriented on the spacecraft such that each sensor viewed a different portion of the celestial sphere during a scan. The spin direction in the B-frame was selected to result in slit crossing geometry I for the three sensors. The inertial spin direction was assumed to be directed near the sun line. Thus, depending on the day of the year, the three sensors observe a predictable number of stars. Assuming that each sensor is sensitive to 4th magnitude stars and brighter (i.e.,  $M_{cm} = 4$ ), Figure 9 indicates the daily number of stars within the field of view of the three sensors.

To provide a range of observed stars, star data were generated for January 12 (dense star day) and for March 7 (sparse star day). In both cases, data were based on the following models of the measurement errors:

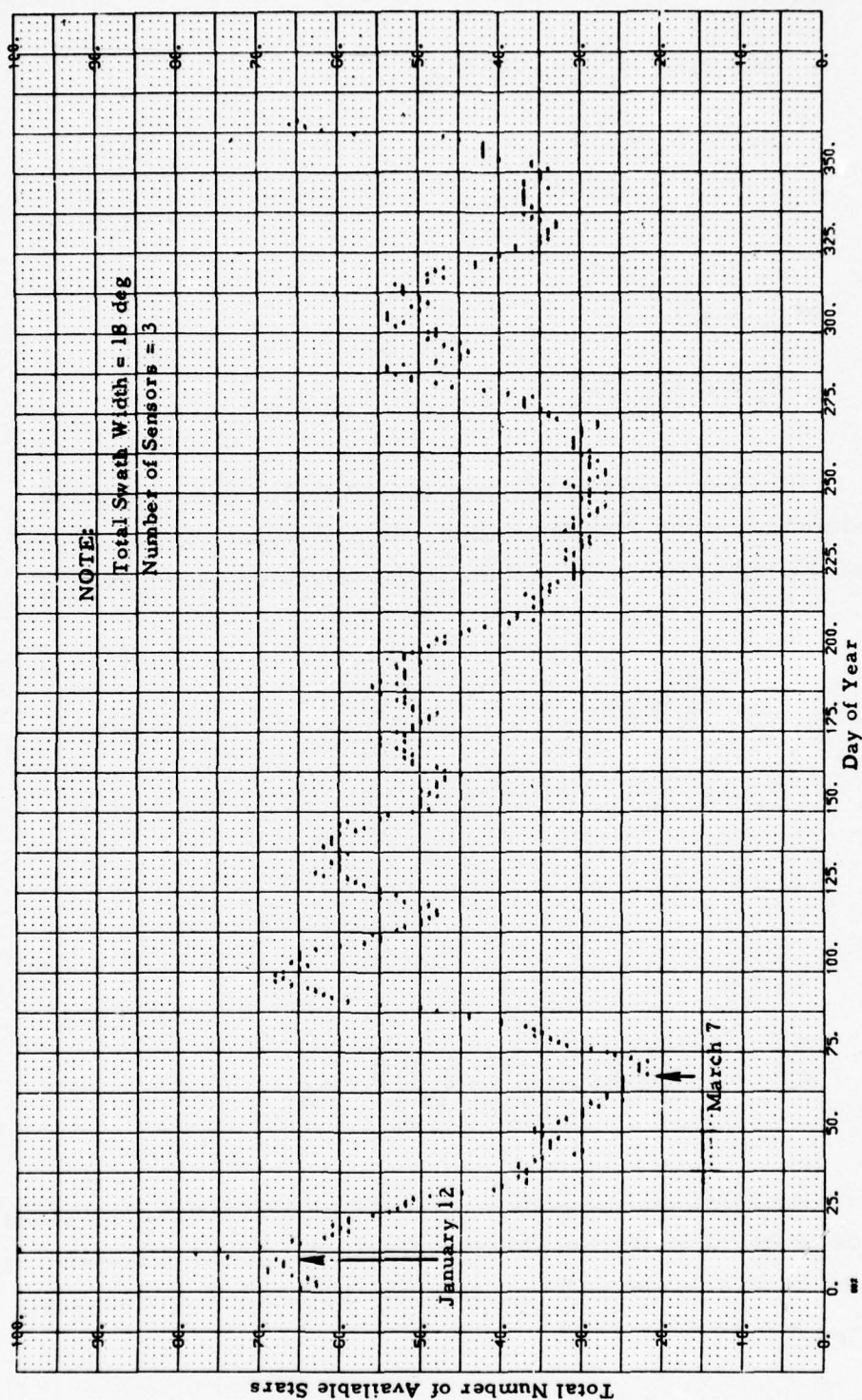


Figure 9. Star Availability versus Day of Year



$$\Delta M = (.01 M_{ij}^{(k)} + .04) M_{cm} \quad (114)$$

$$\sigma_t = 6 \times 10^{-3} T_s \quad (115)$$

where

$$M_{cm} = 4 \quad (116)$$

$$T_s = 2 |\delta_{3j}| / \omega_0 \quad (117)$$

Parameters used by the star identification program were mismodeled from the simulated data. In particular, the program modeled the spin rate as  $\omega_0$  and the error covariances  $P_\Theta$  and  $P_\tau$  as

$$P_\Theta = \sigma_\Theta^2 I_{9 \times 9} \quad (118)$$

$$P_\tau = \sigma_\tau^2 I_{4 \times 4} \quad (119)$$

where

$$\sigma_\Theta^2 = 0 \quad (120)$$

$$\sigma_\tau^2 = \sigma_t^2 + \left( \frac{\Delta \omega_0}{\omega_0} \right)^2 \left( t_{ij}^{(l)} - t_{ij}^{(k)} \right)^2 + \sigma_{tD}^2 \quad (121)$$

Given the star data, the program operated with and without the visual magnitude tests. For the transit time tests, the decision thresholds were selected to achieve a .99 probability of correct decision (i.e.,  $C_{DB} = C_{AB} = 6.635$ ).

## B. RESULTS

The results of the star identification runs are summarized in Table I. The table indicates that no slits or stars were incorrectly identified for the range of parameters considered. Some stars were not identified because of single transits and densely-spaced multiple transits with similar visual magnitudes. Without the visual magnitude tests, the program's capability to discriminate between densely-spaced data was further impaired. Also nutation tended to reduce the number of identified stars.

The rejection of densely-spaced transits with similar magnitudes occurred during the screen operation to avoid multi-star crossing ambiguities. This result implies that there is a star density limit above which no stars will be identified by the method. This limit can be approximated by requiring that the star density  $d_s$  be no more than 1 star per area covered by the field of view, or

$$d_s \leq d_{sm} \quad (122)$$

where

$$d_{sm} = 1/A_F \quad (123)$$

$$A_F = \frac{129600}{2\pi} (1 - \cos F_U) k_F \quad (124)$$

and  $k_F$  is a geometry shape parameter.

Based on stars from the SAO catalog, the star density in stars/square degree brighter than  $M_c$  are plotted against the visual magnitude  $M_c$  are plotted in Figure 10.<sup>(5)</sup> Curves are given for the average density as well as the densities at the extreme galactic latitude bands. Superimposed are levels of  $d_{sm}$  based on a square shape area ( $k_F = 2/\pi$ ) for various field of view angles  $F_U$ . It is noted that as the field of view increases, the screen operation without visual magnitude discrimination tends to reject dim star data. Thus for data processing

Table I. Star Identification Results

Run Conditions				Total Number of Multiple Transit Groups			Total Number of Processed Stars		
Day	Spacecraft Motion	Tests on Visual Magnitude	Total Number of Stars/Scan	Correctly Identified	Incorrectly Identified	Not Identified	Correctly Identified	Incorrectly Identified	Not Identified
March 7	A	Yes	24	21	0	3	21	0	3
	A	No	24	19	0	5	19	0	5
	B	Yes	24	22	0	2	18	0	6
January 12	A	Yes	65	36	0	29	36	0	29
	A	No	65	22	0	43	22	0	43
	B	Yes	65	37	0	28	33	0	32

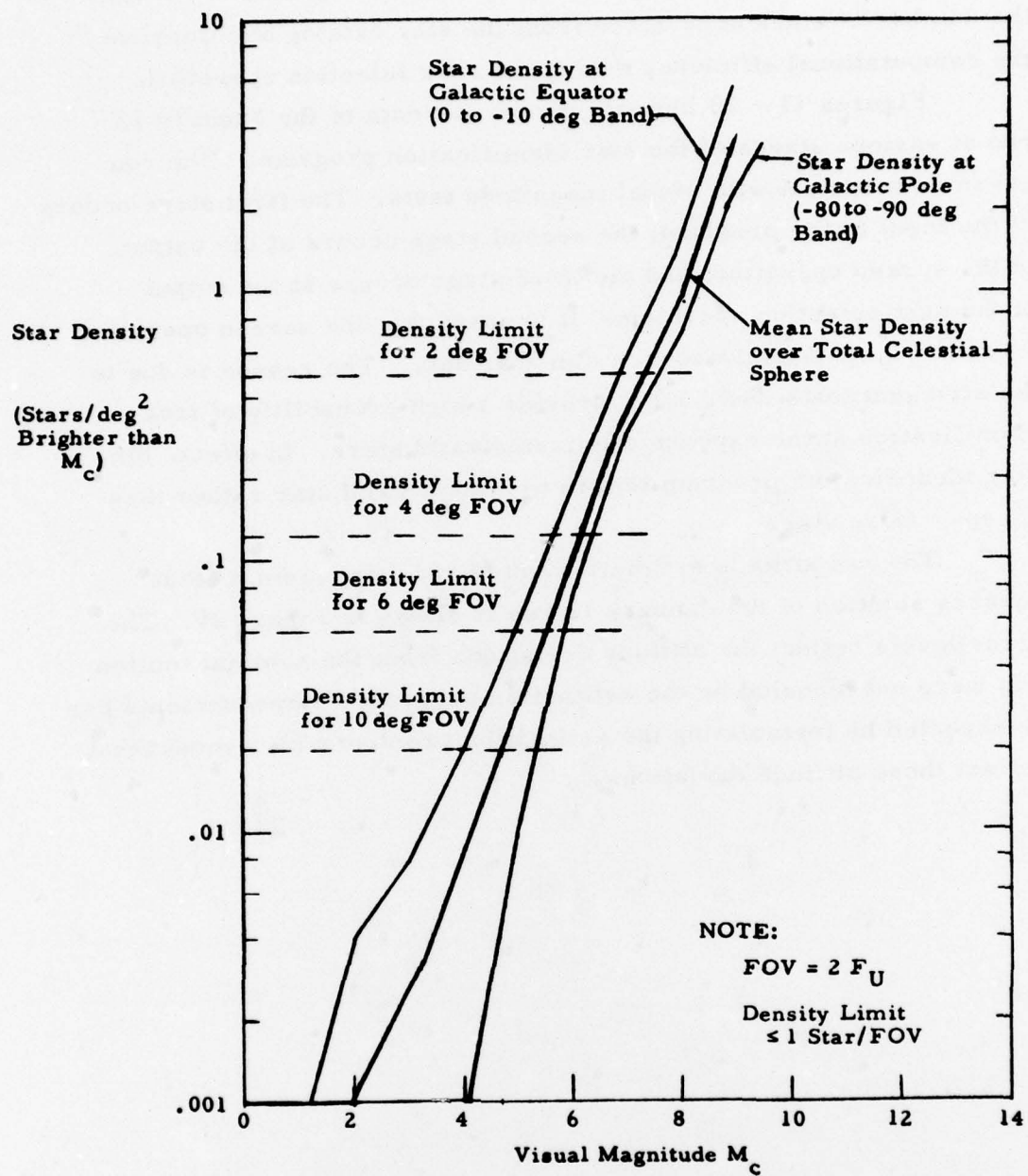


Figure 10. Star Density versus Visual Magnitude



purposes, the visual magnitude parameter  $M_{cm}$  can be reduced to be consistent with the level of Figure 10. This reduction will limit the number of stars considered from the star catalog and improve the computational efficiency during the star selection operation.

Figures 11 - 19 indicate the transit data of the January 12 run at various stages of the star identification program. The run assumed motion A with visual magnitude tests. The first stage occurs at the input to the program; the second stage occurs at the output of the screen operation; and the third stage occurs at the output of the star selection operation. It is noted that the screen operation tends to reject densely-spaced dim star data. The reason is due to the stringent tests designed to provide a high probability of true identification at the expense of missing valid stars. In effect, the star identification program tended to miss a valid star rather than accept a false star.

The rss attitude estimation error resulting from a least squares solution of the January 12 run is shown in Figure 20. The error levels reflect the attitude deviations from the nominal motion that were not modeled by the estimation program. Improvements can be expected by formulating the estimation problem with a model that reflect these attitude deviations.

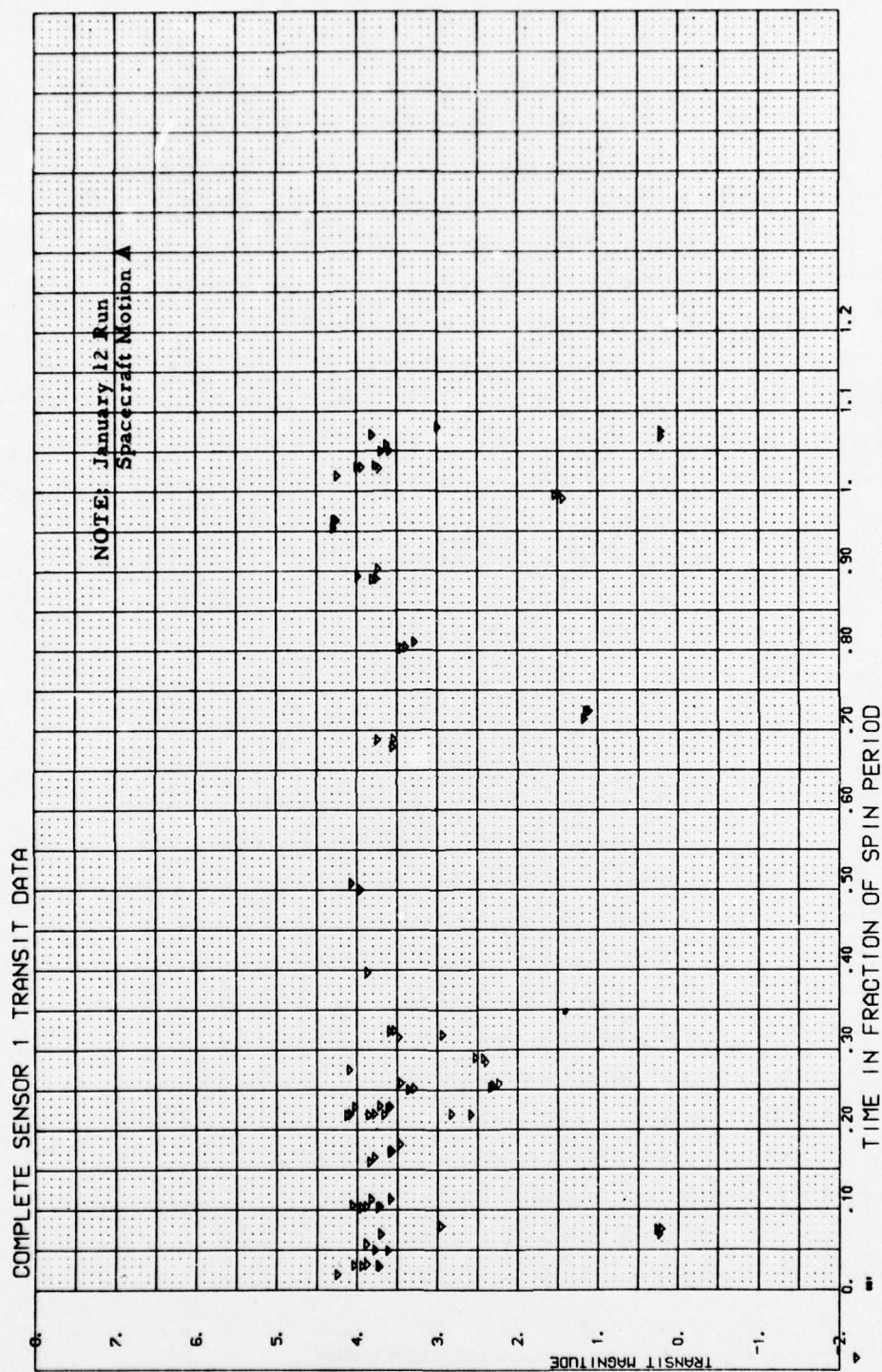


Figure 11. Input Transit Data (Sensor 1)

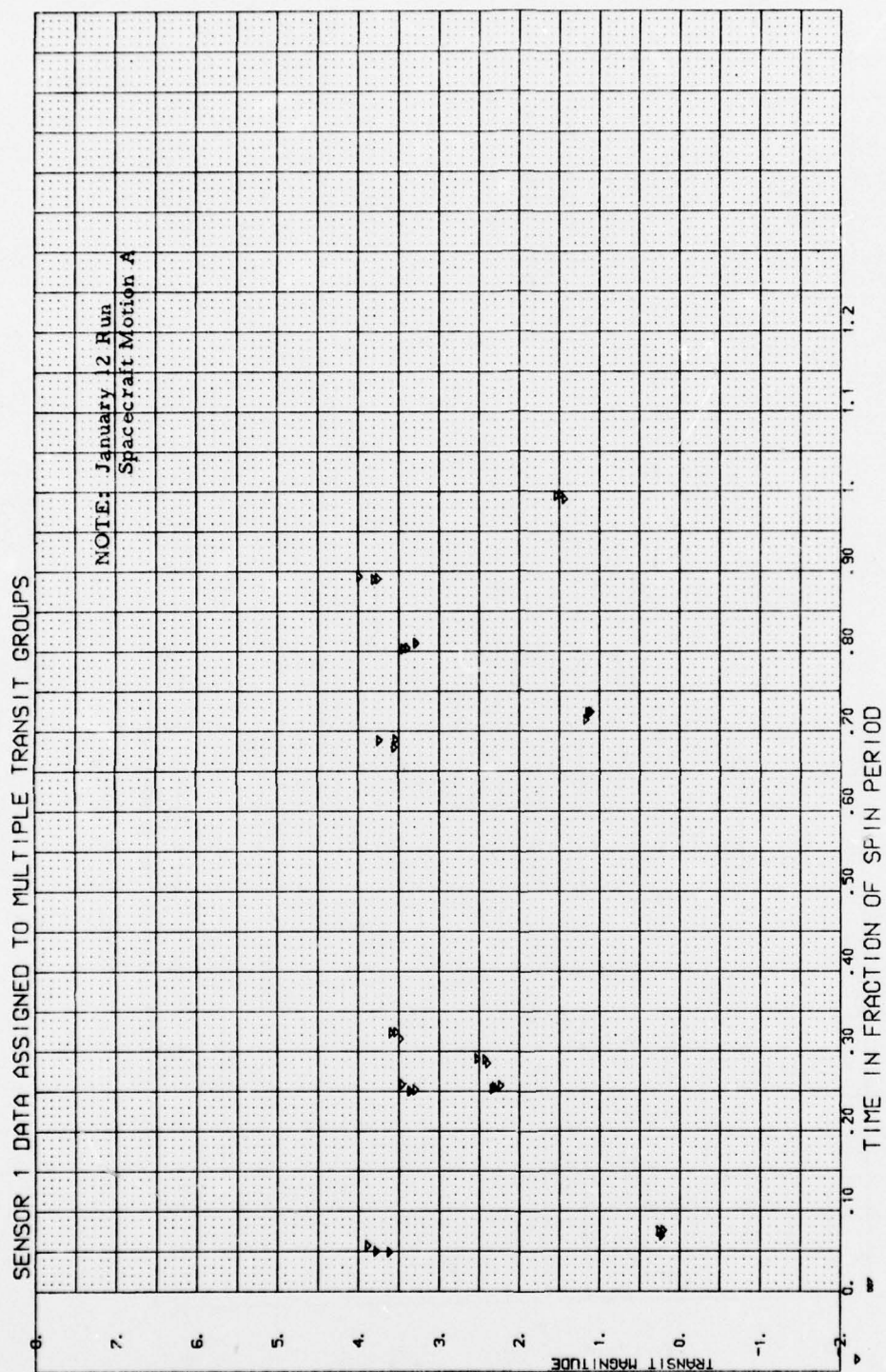


Figure 12. Transit Data Passing the Screen Operation (Sensor 1)



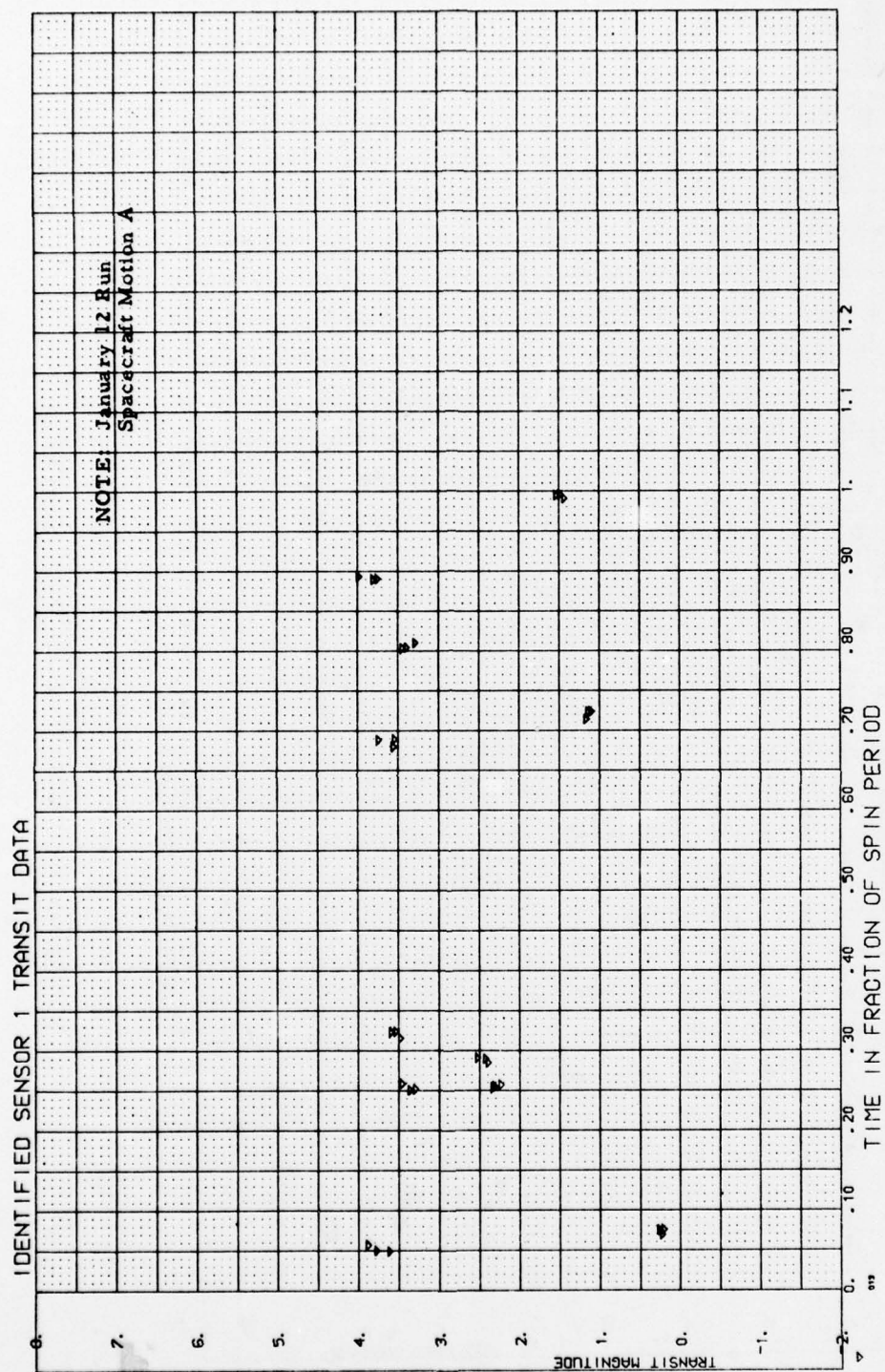


Figure 13. Transit Data Passing the Star Selection Operation (Sensor 1)



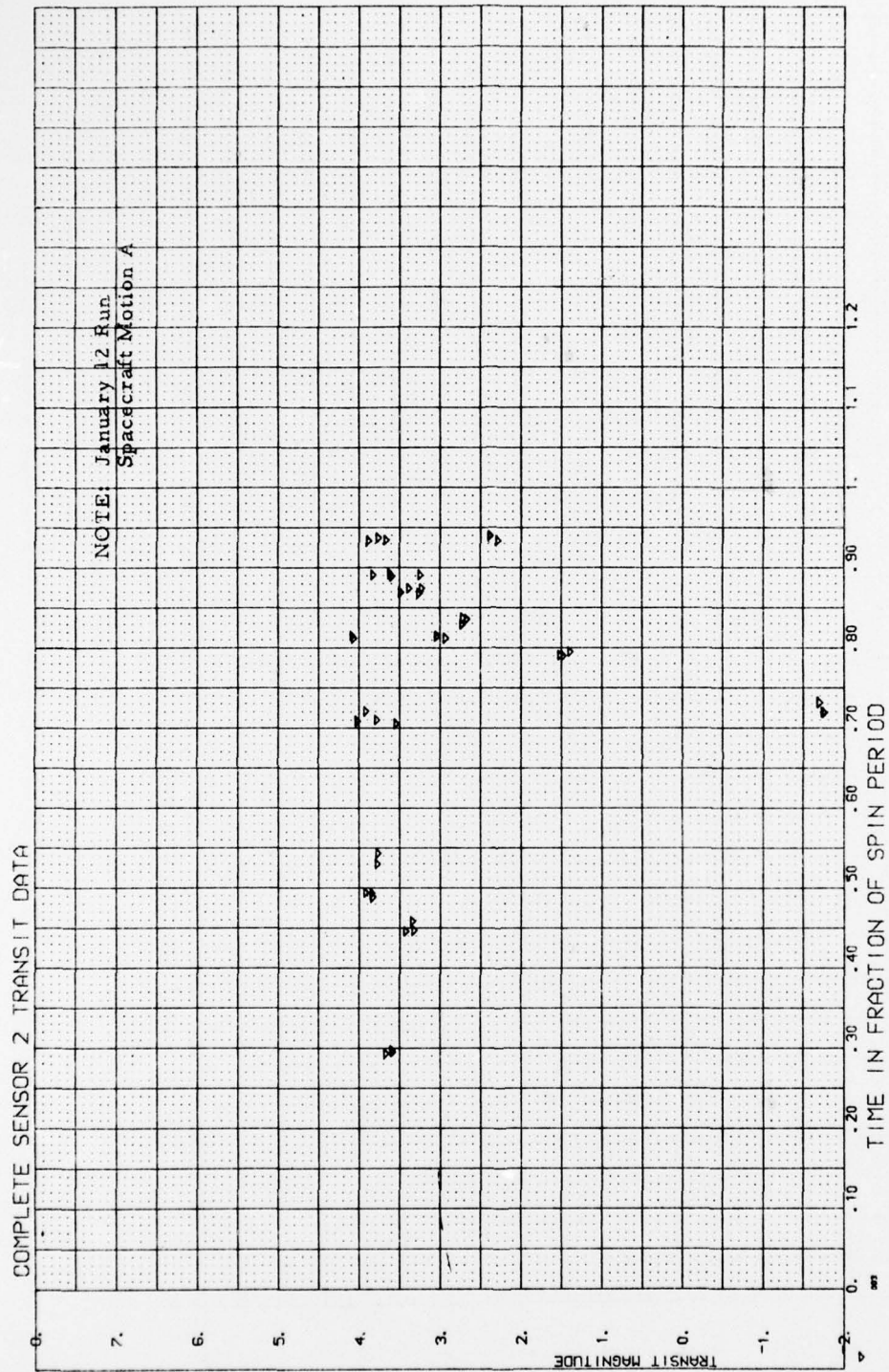


Figure 14. Input Transit Data (Sensor 2)

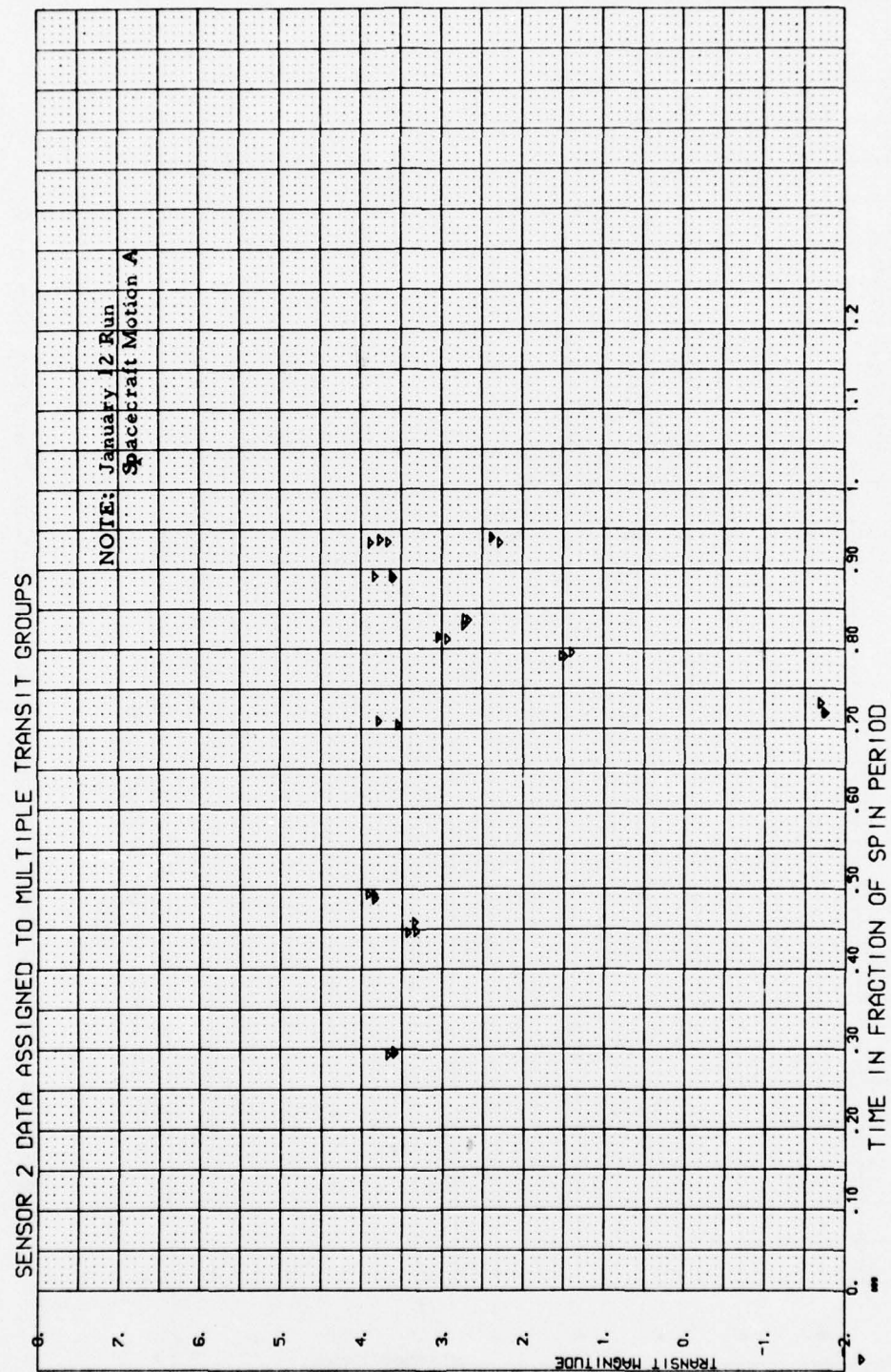


Figure 15. Transit Data Passing the Screen Operation (Sensor 2)

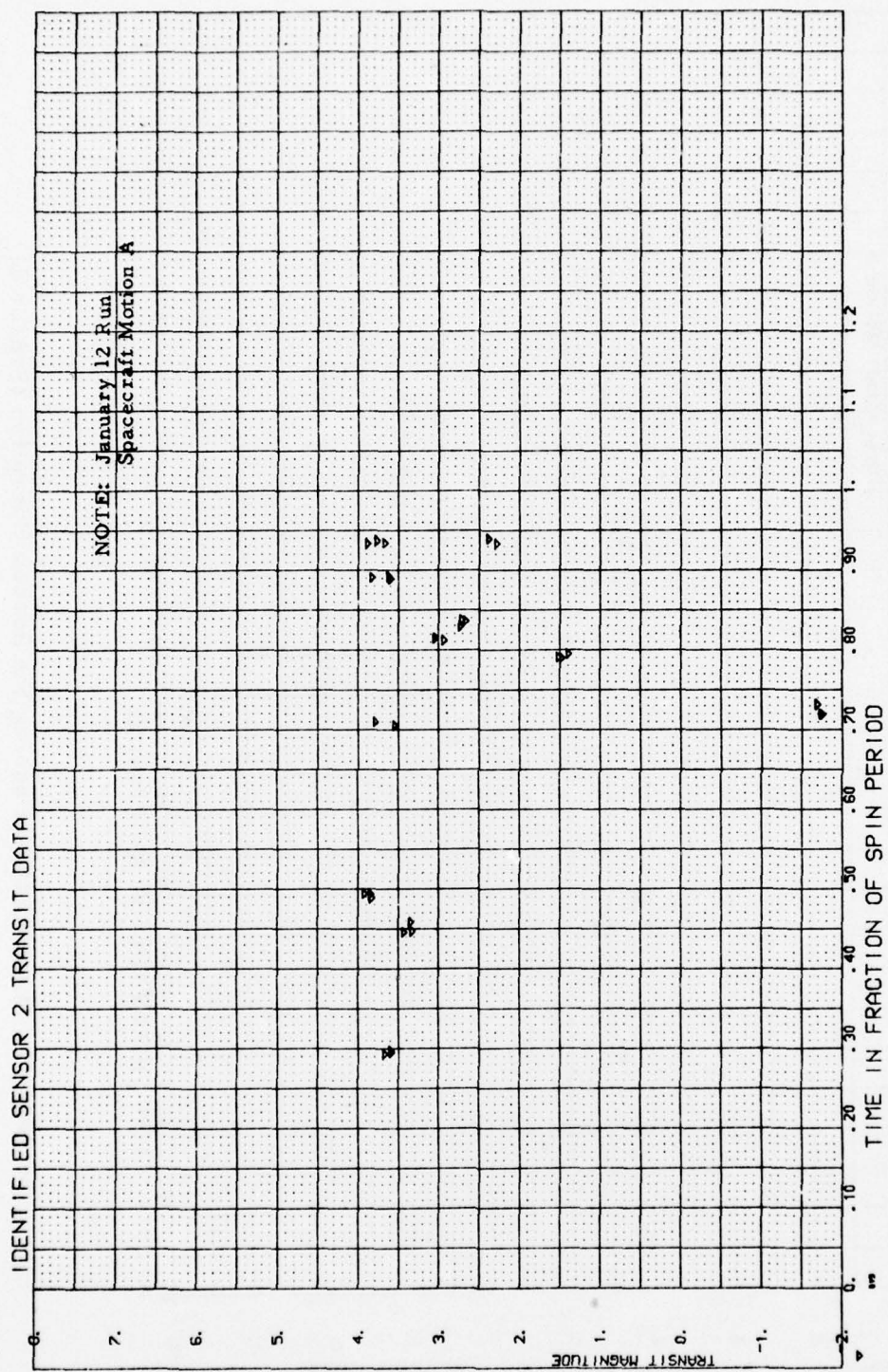


Figure 16. Transit Data Passing the Star Selection Operation (Sensor 2)



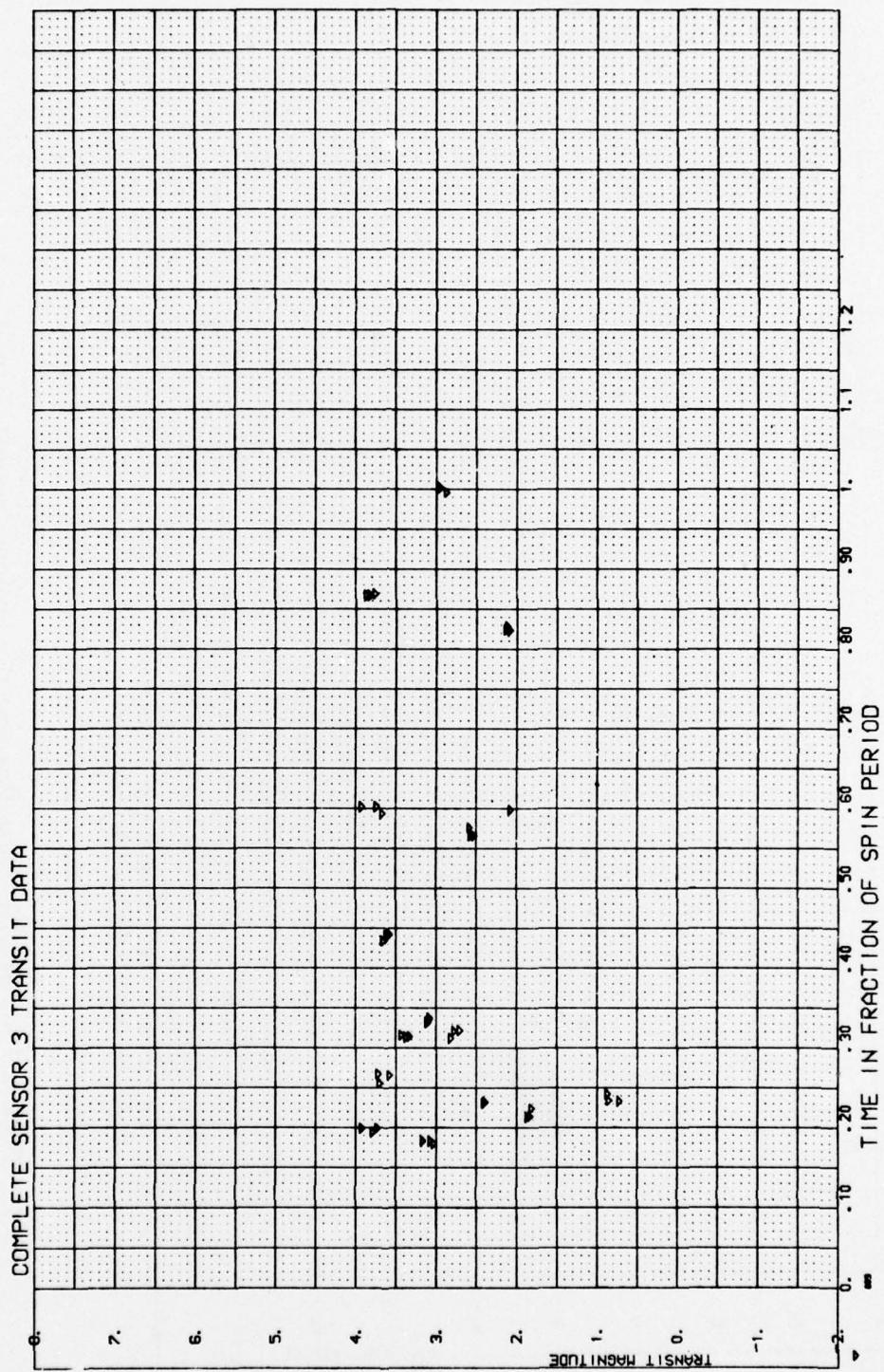


Figure 17. Input Transit Data (Sensor 3)



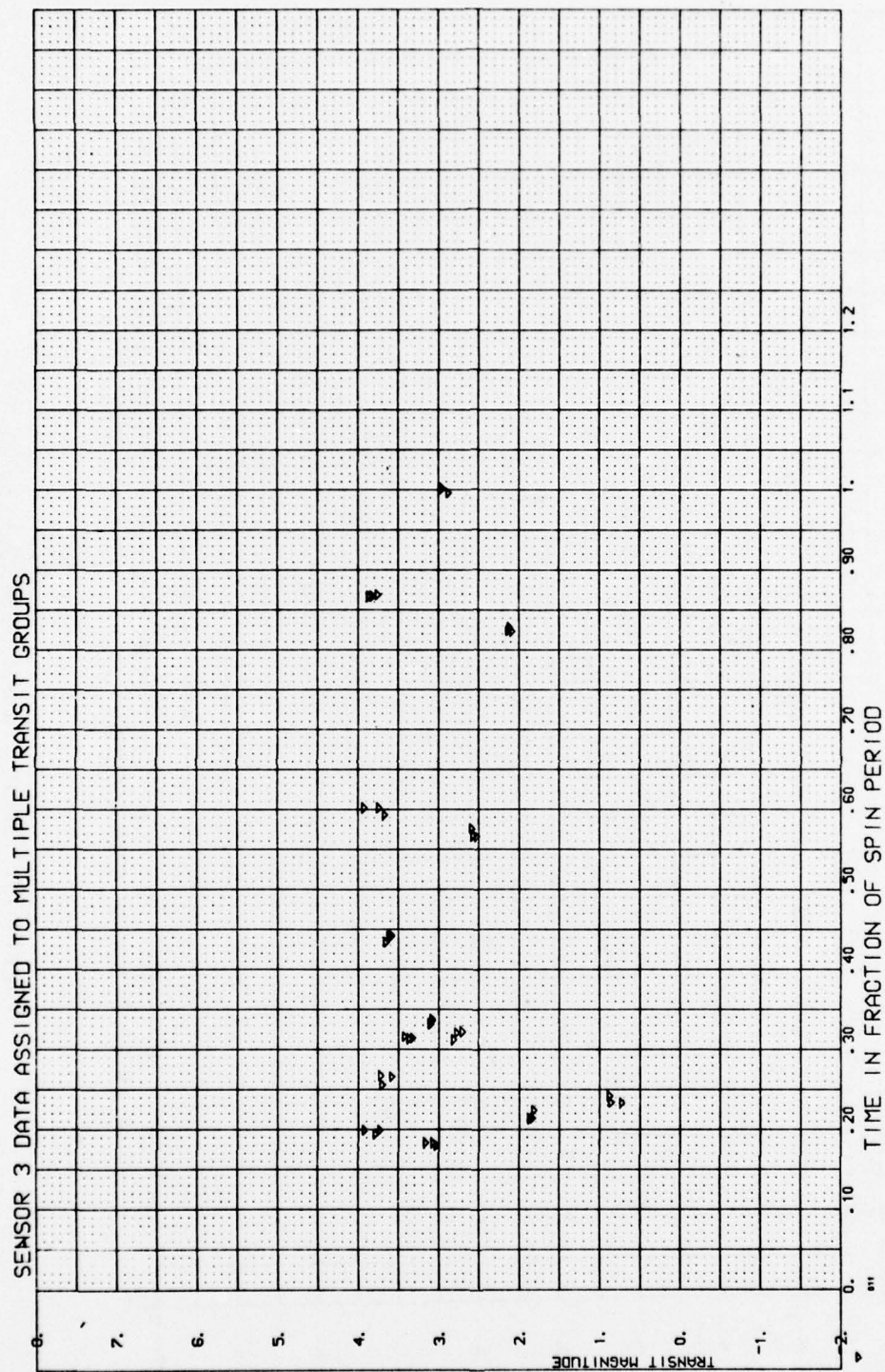


Figure 18. Transit Data Passing the Screen Operation (Sensor 3)

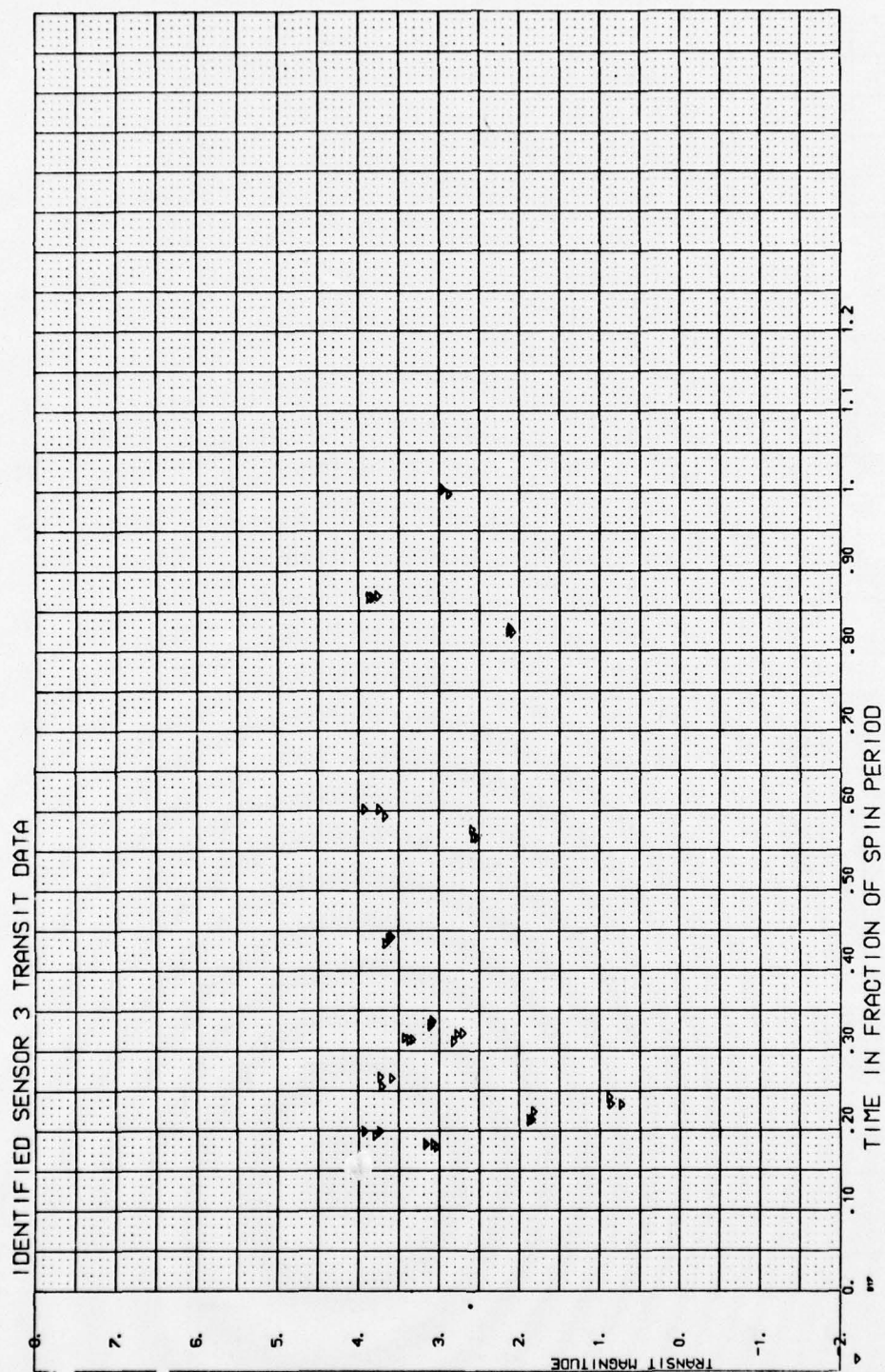


Figure 19. Transit Data Passing the Star Selection Operation (Sensor 3)

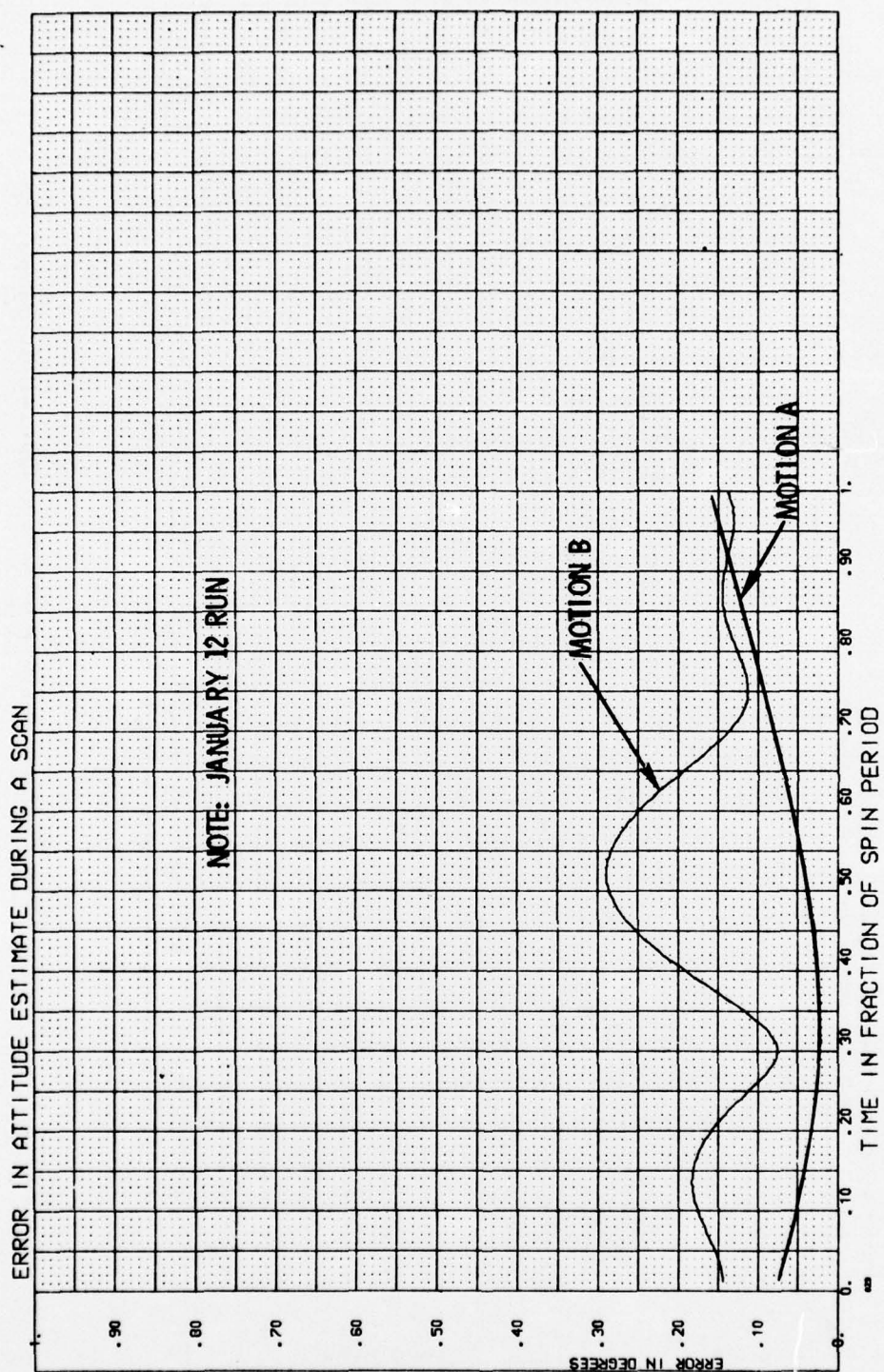


Figure 20. Attitude Estimation Error



## VIII. SUMMARY AND CONCLUSION

The paper has presented a method to identify stars and slits associated with the outputs of star mappers whose inertial orientation is not known. The approach assumed that star data are obtained as the spacecraft performs a spinning maneuver about a known body direction but an unknown inertial direction. Given a known orientation of the star mappers relative to the spacecraft's body frame, expressions were developed to predict the relative transit times between successive slit crossings and to describe the arc length between stars. First-order effects of modeling and measurement errors on the resulting expressions were obtained to provide a statistical basis for slit and star identification. Also a least-squares procedure was outlined to estimate the attitude of the spacecraft based on the identified star data.

A preliminary numerical study indicated that the star identification method is feasible for a limited range of star density. Because high star densities increase the possibility of multi-star crossing ambiguities, the method tended to reject dim stars from consideration. However, those stars that were processed were correctly identified for the range of parameter considered.



## REFERENCES

1. R. L. Kenimer and T. M. Walsh, "A Star Field Mapping System for Determining the Attitude of a Spinning Probe," Paper presented at the Aerospace Electro-Technology Symposium of the International Conference and Exhibit on Aerospace Electro-Technology, April 19-25, 1964.
2. C. B. Grosch, "Orientation of a Rigid Torque-Free Body by Use of Star Transits," AIAA Journal of Spacecraft and Rockets, 4 (5), 562-566 (May 1967).
3. C. B. Grosch, A. E. La Bonte, and B. D. Vannelli, "The SCNS Attitude Determination Experiment on ATS-III," Proceedings of the Symposium on Spacecraft Attitude Determination, September 30 - October 1-2, 1969, 207-221 (31 October 1969).
4. Standard Mathematical Table, 14th Edition, ed. S. M. Selby, The Chemical Rubber Company, Cleveland, Ohio, 270-271 (1965).
5. J. D. Gilchrist, Final Report on Project STRETCH (Space Technology Requirements and Engineering Tests of Components Hardware), Vol. III, TR-0066(5763)-1, The Aerospace Corporation, El Segundo, California (July 31, 1970).